MEASURING RADON CONCENTRATION USING FILTERED AIR SAMPLES

By

Bemenet Alemayehu

A THESIS PRESENTED TO

THE SCHOOL OF GRADUATE STUDIES
ADDIS ABABA UNIVERSITY

IN PARTIAL FULFILLMENT OF THE REQUIREMENTS
FOR THE DEGREE

MASTER OF SCIENCE in PHYSICS

ADDIS ABABA, ETHIOPIA

JULY 2006

ADDIS ABABA UNIVERSITY

SCHOOL OF GRADUATE STUDIES

MEASURING RADON CONCENTRATION USING FILTERED AIR SAMPLES

By

Bemenet Alemayehu

Deaprment of Physics

Addis Ababa University

Approved by the Examining Board:

Dr. Tilahun Tesfaye	Advisor	_____
A.K. Chaubay (Professor)	Examiner	_____
Araya Asfaw (Assoc. Professor)	Examiner	_____

Dated: July 2006

This Work is Dedicated to

A.M.B.Y.F.T.

Table of Contents

List of Tables

List of Figures

Acknowledgements

All have a share in the make up of this thesis but if someone has to be put at the top of the list it shall unmistakably be Dr. Tilahun Tesfaye. He has got everything to do with the flesh and bone of my thesis through his involvement in all my endeavors in the experimental work. I also find it praiseworthy to say that the personal insight and wisdom I learnt from him are as treasured, if not more, as the genius of his teachings. My thanks are many.

Equally helpful had been Dr. Z. Papp of Kossuth University of Budapest, Hungary, especially in his kind assistance of providing us the computer programme designed to calculate the detection efficiency and determination of the Rn isotopes and progeny concentration. I am hugely grateful.

I wouldn't let this opportunity escape without saying 'thank you' for the priceless love, care and encouragement I have received from my parents. The contribution of mom and dad has been, as always, incomparable and beyond mere praise. My thesis would simply have not been as it is now if it were not for them and the earnest support of my sisters and brother. My thanks are heartfelt.

I would also like to express my undivided thanks to my friends and relatives with whom I have shared some great times and obtained a rewarding success.

Addis Ababa University Bemenet Alemayehu

July, 2006

Abstract

Suction pump was used to pass a known volume of air through Whatman® glass fiber filter (> 90 % filtration efficiency). Aerosols deposited on the filter were placed under end-window GM tube with in a minute after the end of sampling, and gross β- count was recorded for successive intervals of time over a period of 7 to 10 hours. The activity concentration of radon daughters was determined by fitting the observed gross β- count to a mathematical model. The diurnal variation of EEC of ^{222}Rn and ^{220}Rn in the nuclear physics lab was observed.

It was found that the highest EEC was during the morning hours and the lowest in the afternoon. The daily average equilibrium equivalent concentrations were 23.9 $\mathrm{Bq/m^3}$ and 5.2 $\mathrm{Bq/m^3}$ for ^{222}Rn and ^{220}Rn respectively.

Chapter 1

Introduction

1.1 Discovery of Radon

Rutherford and R.B.Owens in 1899 noticed that some of the radioactivity of thorium compounds could be blown away. They were studying the emanations from thorium and wrote that the radiation from thorium was not constant but varied in a sudden unexpected changes. Rutherford made the key observations such that, the emanation acts like an ordinary gas and that the intensity of radiation has fallen to one half of its value after an interval of about one minute. Rutherford and Owens had discovered ^{220}Rn (Thoron), half life 51 sec.

Pierre and Marie curie, studying emanations from radium in 1899, concluded that it stayed radioactive for several days. The Curies had detected ^{222}Rn, half life 3.8 days, but they still had doubts as to whether the activity was really in the form of a gas. Later work by Rutherford (1901) and also by Ernst Dorn (1900) confirmed that the radiations emitted by radium were a radioactive gas. It was named 'niton' (Latin root , meaning 'shining') in 1908 by Ramsay and Gray, but soon after came to be called radium emanation, being identified as a radioactive noble gas produced by the decay of radium; it was only since 1923 that it came to be called radon [Nagaratnam, 1994].

Actinon, another isotope of radon, was discovered in 1904 by Friedrich Giessel and Andre-Lousi Debierne. Inadditon to the above mentioned three naturally occurring isotopes, another around 17 isotopes of radon are known.

The first radon measurements were made in 1901 [Nagaratnam, 1994] by

Elster and Geitel. These revealed that radon is a ubiquitous constituent of atmospheric air. The early environmental measurement of radon were done for the study of diverse phenomena such as atmospheric electricity, atmospheric transport, and exhalation of gases from soil.

1.2 Physical properties of radon

Radon is a unique natural element in that it is the only radioactive and noble gas. It is one of the heaviest gas at room temperature and chemically inert.

At standard temperature and pressure radon is a colorless gas but when it is cooled below its freezing it has a brilliant phosphorescence which turns yellow as the temperature is lowered and orange-red at the temperature air liquifies.

Physical properties of radon	
Name , Symbol , Number	radon , Rn , 86
Chemical series	noble gases
Group , Period , Block	18 , 6 , p
Appearance	colorless
Atomic mass	(222) g / mol
Electron configuration	[Xe] $4f^{14}$ $5d^{10}$ $6s^2$ $6p^6$
Electrons per shell	2,8,18,32,18,8
Phase	gas
Melting point	202 °K (-71 °C)
Boiling point	211.3 °K (-61.7 °C)
Heat of fusion	3.247 KJ / mol
Heat of vaporization	18.10 KJ / mol
Heat capacity	(25 °C) 20.786 J / (mol . °k)

Table 1.1: Physical properties of Radon

1.3 Sources of radon

Radon is an ubiquitous element found worldwide. Radon is produced by the radioactive decay of radium which is a member of the naturally occurring Uranium decay series. The most abundant isotope ^{222}Rn is a descendant of ^{238}U while ^{220}Rn (thoron) and ^{219}Rn (actinon) are the descendants of ^{232}U and ^{235}U respectively.

There are around seventeen known isotopes of radon. The decay series of the three abundant isotopes is shown below.

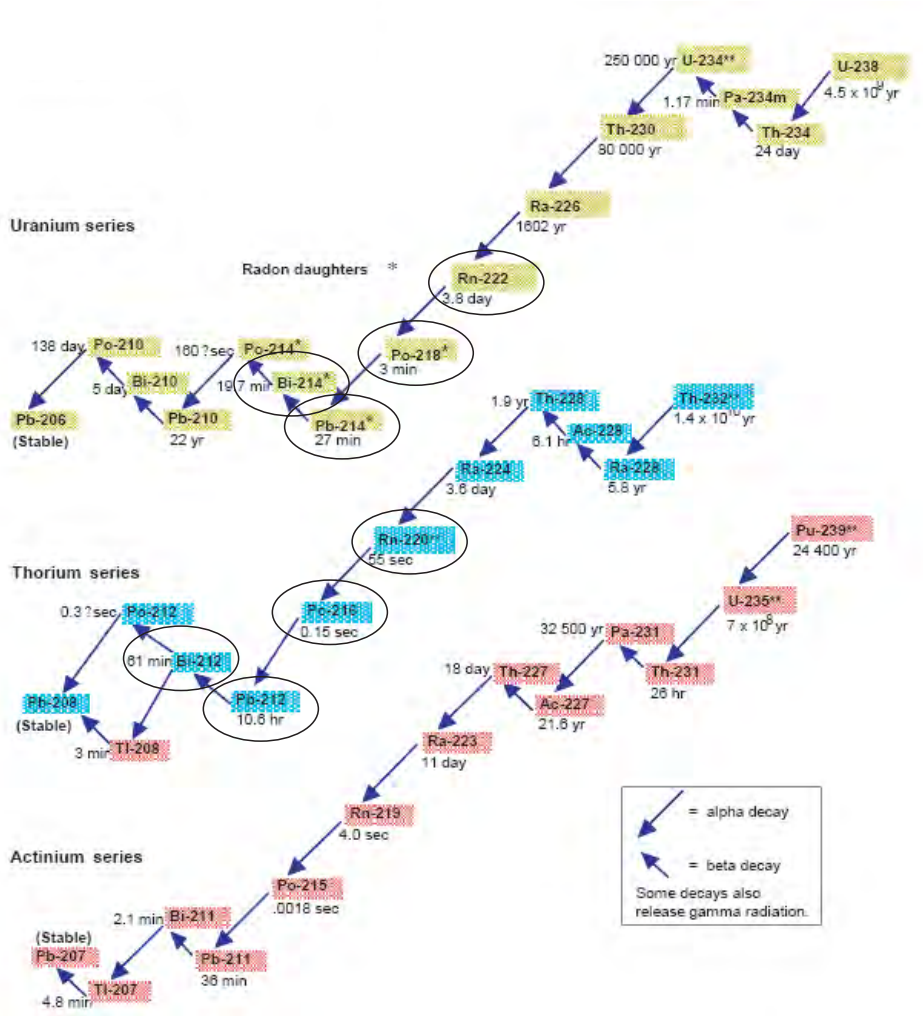

Figure 1.1: Decay series of Radon isotopes

1.3.1 Radon entry into the atmosphere

^{222}Rn and ^{220}Rn are the gaseous radioactive products of the decay of the radium isotopes ^{226}Ra and ^{224}Ra which are present in all terrestrial materials. Some of the atoms of these radon isotopes are released from the solid matrix of the material by recoil when the radium decays.

For a radon atom to escape from the mineral grain into the pore space, the decay must occur within the recoil distance of the grain surface. The range of

recoil distance for ^{222}Rn is 20-70 nm in common minerals, 100 nm in water, and 63 μm in air [UNSCEAR, 2000]. Radon atom entering the pore space are then transported by diffusion and advection through this space until they in turn decay or are released into the atmosphere (exhalation). Radon generation and transport in porous materials involve solid, liquid, and gas phase in the process of emanation, diffusion, advection, absorption in the liquid phase, and adsorption in the solid phase.

The fraction of radon atoms released into rock or soil pore space from a radium-bearing grain is called the *emanation coefficient*, the *emanation factor* or the *emanating power*. Grain size and shape are two important factors that control the emanation of radon in soil.

Microscopic fractures and fissures, called nanopores, and pits or openings caused by previous radioactive decays provide additional pathways for radon release. Particularly in sand-sized and larger grains, nanopores can increase the specific surface area of the grain, enhancing emanation by one or two orders of magnitude.

Soil moisture plays an important role in the emanation of radon and its diffusion in soil for several reasons. Soil moisture, in the form of a thin film of water surrounding soil grains, directly affects radon emanation by capturing the radon that recoils from the solid matrix. These captures increase the likelihood that radon atom will remain in the pore space instead of crossing the pores and imbedding themselves in adjacent soil grains.

The main mechanism for the entry of radon into the atmosphere is molecular diffusion. Although diffusive entry of radon into the outdoor atmosphere usually dominates, there is also some advection caused by wind and changes in barometric pressure. Measurements of exhalation rates of radon from soil show a variability of radon concentrations in near surface pore spaces. Concentrations of ^{222}Rn in soil gas vary over many orders of magnitude from place to place and show significant time variations at any given site. Data have shown that there were prominent increases in radon concentrations in outdoor air and in ground water just before the larger earthquake at Kobe, Japan in 1995 [UNSCEAR, 2000].

Under normal circumstances, thoron concentrations in soil gas would be roughly comparable to or perhaps somewhat less than the ^{222}Rn concentrations because of the generally similar production rates in rocks and soils and their behavior

in the ground. On the other hand, high thoron entry rates from the ground are rarely encountered. Whereas fractures in the ground and/or bedrock allow ^{222}Rn to be pulled to the surface from substantial depths (and volumes), the time frame may be such that most of the thoron present at these depths decays before reaching the surface.

1.3.2 Radon in mines

Radium available as part of the ore is the major source of radon in mines. Production and release into the mine atmosphere depends on the grades, its emanation power, porosity and permeability of host rock to radon and moisture content of the ore. Water coursing through the ore body remains under high pressure which dissolves significant amounts (up to 23%) of radon available in the ore spaces through which it passes; this acts as an efficient medium of transport for radon carrying it from far-off places and discharging it into the mine cavity. The moment radon-laden water enters the mine openings and flows through the mine galleries, dissolved radon is released due to depressurization and constant agitation. [UNSCEAR, 2000]

Radon produced by the decay of radium located in the grains of the ore matrix moves out by recoil into the pore spaces and remains locked up there. Mining operations such as drilling and blasting bring fresh radon into the mine air.

Radon gas, on entering the mine air by various processes remains there till it is carried along in the ventilation current and discharged above ground. Because of its comparatively long half life (3.8 days) compared with the residence time of air in a mine (approx. 40 mins.), radon concentration increases in proportion to its rate of release and travel time along different passages of the mine. [UNSCEAR, 2000]

1.3.3 Radon in outdoor air

Concentrations of radon in the outdoor environment are affected not only by the magnitude of the exhalation rates in the general area but also by atmospheric mixing phenomena. Solar heating during the daytime tends to induce some turbulence, so that radon is more readily transported upwards and away from the ground. At night and in the early morning hours, atmospheric (temperature) inversion

conditions are often found, which tend to trap the radon closer to the ground. This means outdoor radon concentrations can vary diurnally by a factor of as much as ten. There are also seasonal variations related to the effects of precipitation or to changes in the prevailing winds. These effects must be taken into account when interpreting the available measurements [UNSCEAR, 2000]

Although data are scarce for thoron, considerable variability from place to place would be expected because of thoron's short half-life. Even more important is the fact that thoron's short half-life results in a very steep vertical gradient in its atmospheric concentration at any location. A few measurements show that concentrations a few centimeters above the ground surface and concentrations at a height of 1 m vary by a factor of about 10. This gradient would be expected to vary considerably with atmospheric conditions. Thus, pronounced time variations would be expected at any height above the ground at any location. [UNSCEAR, 2000]

1.3.4 Radon in indoor air

Exposure to the short-lived daughters of radon is not confined to the underground miners. Uranium is widely distributed constituent of the earth's crust, typically in 2–4 parts per million and in consequence is found in most materials commonly used by the building industry. Radon, being a noble gas, diffuses from the subsoil below the building into room air, where it and its daughters are available for inhalation by the room occupants [Cliff, 1978].

The early recognition of radon as a carcinogen in the 1920s did not initiate investigation in dwellings until much later. There were two main reasons for the long long delay. Firstly, the carcinogenicity of radon miners was not generally accepted and secondly, much lower radon levels were expected in dwellings above ground [Cliff, 1978].

In the early years of the 20th century, the newly discovered thorium and radium emanation (i.e. thoron and radon), the active deposit (radon daughters) and radium itself were investigated in laboratories in more detail.

Outdoors, where it is diluted to low concentrations in the air, ^{222}Rn poses significantly less risk than indoors. In the indoor environment, however, ^{222}Rn

can accumulate to significant levels. The magnitude of ^{222}Rn concentration indoors depends primarily on the type of construction materials of the building and the amount of uranium deposition in the underlying soil. The soil composition under and around a house affects ^{222}Rn levels and the ease with which ^{222}Rn migrate into a house. Normal pressure differences between the house and the soil can create a slight under pressure in the house that can draw ^{222}Rn gas from the soil into the building. ^{222}Rn moves more rapidly through permeable soils, such as coarse sand and gravel , than through impermeable soils, such as clays. Fractures in any soil or rock allow ^{222}Rn to move more quickly. In a very small number of houses ^{222}Rn levels are generally highest in basements and ground floor rooms that are in contact with the soil. Factors such as design, construction, and ventilation of the house affect the pathways and sources that can draw ^{222}Rn indoors [Tassos and Haralabos, 2003].

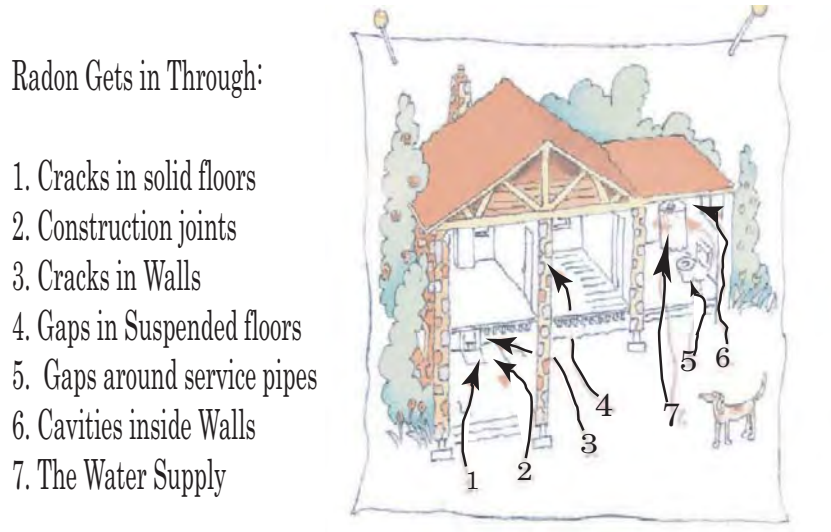

Figure 1.2: Radon entry into the house [EPA, 2005]

The chances of increased level of indoor radon is higher in areas of higher uranium laden soil. But some houses in areas with lots of uranium in the soil have low levels of indoor ^{222}Rn, and other houses on uranium-poor soils have high levels of indoor ^{222}Rn. Clearly, the amount of ^{222}Rn in a house is affected by other factors in addition to the presence of uranium in the underlying soil. One example is the permeability of the soil [Tassos and Haralabos, 2003].

Considering all of the factors mentioned above, and especially the design and

quality of construction of an individual structure, the factors that determine the entry rate are many, varied, and very site-specific. Successful mitigation strategies, such as identifying and sealing a limited number of entry pathways or effectively ventilating the soil immediately adjacent to the foundation, tend to work because radon entry into structures can be fairly readily prevented, or at least substantially reduced, be redirecting and re-channelling air transport away from building interiors. Radon concentrations are typically reduced by about 30 percent. Other techniques aim at reducing the building/ground pressure differential that drives the advection; the radon convections are typically reduced by 80-90 percent. Improvements in ventilation systems normally change radon concentration by less than 50 percent [UNSCEAR, 2000].

The processes that may allow thoron to accumulate in indoor air are difficult to assess. Because of thoron's short half-life, it was once thought that the only mechanisms for significant thoron entry would be infiltration of outdoor air diffusion from building materials. But recent investigations have shown that entry through the foundation can also be important. There is an absence of detailed studies in a sufficiently large sample of buildings to make wide generalizations. However, given the comparable concentrations of ^{222}Rn and ^{220}Rn usually found in outdoor air, soil gas, and building material pore spaces, it is not unexpected that indoor air concentrations of the two gases (ground floor level only) are often roughly comparable [UNSCEAR, 2000].

Many of the studies of ^{222}Rn and ^{220}Rn source terms have dealt with single-family houses with or without basements and crawl spaces. There is less information on multi-storey buildings, such as apartment houses and office buildings. The expectation that ground sources would be less important for spaces well above the ground has generally been supported by lower concentrations of ^{222}Rn and ^{220}Rn in higher stories [UNSCEAR, 2000].

Studies show that radon the concentration of radon gas is decreases with the elevation above the ground level i.e. ground floors have higher concentration as compared to higher stories. Similarly, factors like ventilation, room usage, building materials also affect the indoor radon concentration [Al-Sharif and Abelrahman, 2001].

Table 1.2: Radon concentrations in dwellings [UNSCEAR, 2000]

Region	Country	Population In 1996 (10^6)	Radon concentration (Bqm^{-3})			
			Arith. mean	Geom. mean	Max. Value	Geom. Standard Deviation
Africa	Algeria	28.78	30		140	
	Egypt	63.27	9		24	
	Ghana	17.83			340	
North America	Canada	29.68	34	14	1720	3.6
	United States	269.4	46	25		3.1
South America	Argentina	35.22	37	26	211	2.2
	Chile	14.42	25		86	
	Paraguay	4.96	28		51	
East Asia	China	1232	24	20	380	2.2
	Honk Kong	6.19	41		140	
	India	944.6	57	42	210	2.2
	Indonesia	200.45	12		120	
	Japan	125.4	16	13	310	1.8
West Asia	Armenia	3.64	104		216	1.3
	Iran(Islamic Rep.of)	69.98	82		3070	
	Kuwait	1.69	14	6	120	
	Syria	14.57	44		520	
North Europe	Denmark	5.24	53	29	600	2.2
	Estonia	1.47	120	92	1390	
	Finland	5.13	120	84	20000	2.1
West Europe	Austria	8.11		15	190	
	Belgium	10.16	48	38	12000	2
	France	58.33	62	41	4690	2.7
	Germany	81.92	50	40	>10000	1.9
Eastern Europe	Bulgaria	8.47		22	250	
	Czech Republic	10.25	140		20000	
	Hungary	10.05	107	82	1990	2.7
South Europe	Albania	3.4	120	105	270	2
	Croatia	4.5	35	32	92	
	Spain	39.67	86	42	15400	3.7
Oceania	Australia	18.06	11	8	420	2.1
	New Zealand	3.6	20	18	90	
Median			46	37	480	2.2
Pop.-weighted average			39	30	1200	2.3

Table 1.3: Thoron concentrations in outdoor and indoor air [UNSCEAR, 2000]

Region / Country	Equilibrium equivalent concentration (Bq m^{-3})		$^{220}Rn/^{222}Rn$ EEC ratio	
	Outdoors	Indoors	Outdoors	Indoors
North America				
United States	0.09 (0.03-0.3)	0.5 (0.03-4.7)		0.04
East Asia				
China	0.4	0.8	0.05	0.07
Hong Kong	0.3 (0.1-0.5)	0.8 (0.4-1.2)	0.04	0.06
Japan	0.09 (0.03-0.12)	0.6 (0.4-0.9)		0.1
Malaysia	0.5 (0.3-1.8)	1.1 (0.4-2.5)	0.08	0.08
North Europe				
Norway		0.7 (0.07-1.1)		0.04
Sweden		0.3 (0.1-0.6)		0.01
West Europe				
France		0.8 (0.6-13.3)		0..03
United Kingdom		0.3 (0.07-1.1)		0.02
Central Europe				
Germany		0.5 (0.1-1.0)		
Moldova	0.2	1.0 (0.1-6.4)	0.04	0.05
Romania	0.3 (0.1-0.6)	1.1 (0.1-6.4)	0.05	0.04
East Europe				
Russia		1.1-7.1		0.09 (0.02-0.24)
South Europe				
Italy		12 (0.5-7.6)		0.11 (0.01-0.38)
Slovenia	0.12 (0.05-0.37)		0.013	
Range	0.09-0.5	0.2-12	0.01-0.08	0.01-0.5

1.3.5 Radon in water

Radon is also found in the water, in homes, in particular, homes that have their own well rather than municipal water. When the water is agitated, as when showering or washing dishes, radon escapes into the air. However, radon from domestic water generally contributes only a small proportion (less than one percent) of the total radon in indoor air. Municipal water systems hold and treat water, which helps to release radon, so that levels are very low by the time the water reaches homes. But people who have private wells, particularly in areas of high radium soil content, may be exposed to high levels of radon [EPA, 2005].

1.4 Health hazards due to radon

1.4.1 Discovery

G. Agricola (1494 - 1555) working in Joachimsthal (now Jachymov), Czechoslovakia, chronicled unusually high mortality from respiratory disease among underground metal miners in the Erz mountains of Eastern Europe. In 1879, autopsy findings that documented pulmonary malignancy in miners in that region was described. By early in the 20th century the malignancy was shown to be primary carcinoma of the lung. The finding of high levels of radon mines in the region and in the nearby mines of Joachimsthal, where miners also had high lung cancer rates, led to the hypothesis that radon was the cause of the lung cancer. That hypothesis was not uniformly accepted until the findings of epidemiologic studies of other groups of radon exposed underground miners were reported during the 1950s and 1960s. Those studies continue to support the implementation of regulatory programs to reduce exposure of underground miners to radon and to provide compensation for occupational lung cancer [National Research Council, 1999].

Some association between cancer and radioactivity had been demonstrated as early as 1902, starting from the first cases of skin cancer induced by x-rays or radium emanation. Since detailed measurements showed a high concentration of radon in the air of mines at Schneeberg and Jachymov, a relation between radon and lung cancer came to be suspected. Probably the first person to suspect this casual line was H.E.Muller, a miner from Saxony. It is interesting to recall that as

early 1907, Lord Rutherford in a lecture in Canada, speculated that the inhalation of radon and progeny may play some part in the physiological processes, but it was no more than a wild speculation. The hypothesis of correlation between lung cancer and radon inhalation was supported by more precise radon measurements carried out in the 1920, leading Ludewig and Lorenzer in 1924 to make a definitive statement of the link. However, this hypothesis was not generally accepted. An expert pathological study group in Germany in its 1926 report ascribed the cancer to inhalation toxic ore dusts [Nagaratnam, 1994].

In 1936 Rajewsky initiated a comprehensive study programme involving radon measurements in Schneeberg mines, measurements of the alpha activity in the tissue samples and histopathological analysis of lung tissues from miners who had died of lung cancer. At that time, the average radon concentration in most mines at Schneeberg was in the range of $70 - 120\,\mathrm{KBqm}^{-3}$. In one time, however, the mean level was $500\,\mathrm{KBqm}^{-3}$, and most workers here died from lung cancer; it was called 'death mine'. On the basis of these studies Rajewsky was able to establish conclusively in 1940 the casual link. However, till 1945, no quantitative dose-response relation could be worked out, nor was the possible role of inhalation of short-lived radon progeny realized [Nagaratnam, 1994].

Although, the progeny of radon are now a well recognized cause of lung cancer, radon itself has again become a topic of controversy and public health concern because it has been found to be a ubiquitous indoor air pollutant to which all persons are exposed. Radon was found to be present in indoor air as exactly as the 1950s, but the potential health implications received little attention until the late 1970s . Arguably, the most significant event to draw the radon problem to the attention of the media and ultimately the public at large were the remarkable circumstances surrounding a person called Stanley Watras and the event is commonly refereed as The Watras incident. Stanley Watras was living in Boyertown, near to Philadelphia, and was an employee of the Limerick Nuclear Power plant in Pennsylvania. The home of the unfortunate Watras was built on an excavated vein of uranium in the Reading Prong, a Precambrian rock body relatively high in uranium. During December 1984, Watras set off radiation alarms on his way into work. This happened every working day for two weeks and he was regularly decontaminated while the authorities attempted to find the radioactive source.

Table 1.4: Average worldwide exposure to natural radiations [UNSCEAR, 2000]

Source of exposure	Average effective dose (mSv) Average	Typical range
Cosmic radiation		
Directly ionizing and photon component	0.28	
Neutron component	0.1	
Cosmogenic radionuclides	0.01	
Total cosmic and cosmogenic	**0.39**	**0.3-1.0**
External terrestrial radiation		
Outdoors	0.07	
Indoor	0.41	
Total external terrestrial radiation	**0.48**	**0.3-0.6**
Inhalation exposure		
Uranium and thorium series	0.006	
Radon (^{222}Rn)	1.15	
Thoron (^{220}Rn)	0.1	
Total inhalation exposure	**1.26**	**0.2-10**
Ingestion exposure		
^{40}K	0.17	
Uranium and thorium series	0.12	
Total ingestion exposure	0.29	0.2-0.8
Total	**2.4**	**1-10**

Eventually, the source was found to be radon gas in his domestic dwelling, not a discharge at the plant itself. The levels of radon in his home appeared astonishing to those monitoring at the time, being in the region of 100 000 $\mathrm{Bqm}-3$. The risks associated with living in that house were estimated to be equivalent to smoking 135 packs of cigarettes per day [National Research Council, 1999].

Radon has now been classified as a human carcinogen by the International Agency for Research on Cancer (IARC). One study by U.S. environmental protection agency [EPA, 2005] showed that radon is estimated to cause thousands of lung cancer deaths in the U.S. each year (see figure 1.3).

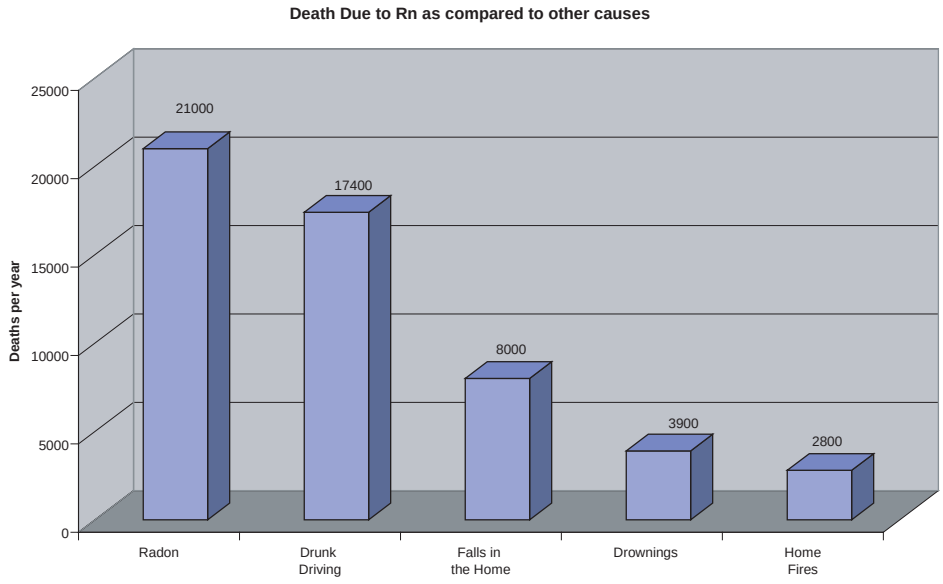

Figure 1.3: Death due to radon as compared to other causes in U.S. [EPA, 2005]

Radon is estimated to cause about 21,000 lung cancer deaths per year, according to EPA's 2003 Assessment of Risks from Radon in Homes. The numbers of deaths from other causes are taken from the Centers for Disease Control and Prevention's 1999-2001 National Center for Injury Prevention and Control Report and 2002 National Safety Council Reports.

1.4.2 Effects of radon on the body

Inhalation is the main route of entry, into human body, for radon and its progeny. [EPA, 2005].

Most of the radon gas inhaled is also exhaled. However, some of radon's decay products attach to dusts and aerosols in the air and are then readily deposited in the lungs. Some of these are cleared by the lung's natural defence system, and swallowed or coughed out [EPA, 2005].

The life time of ^{222}Rn is long relative to breathing times. Most of it that is inhaled is exhaled again rather than decaying or becoming lodged in the lungs and later decaying. In contrast, the immediate, promptly decaying daughters of ^{222}Rn: (^{218}Po, ^{214}Pb, ^{214}Bi, and ^{214}Po) attach to a surface, typically of aerosols, which can be inhaled. They then deposit on epithelial surfaces within the lung, and shortly decay. The result is that the sensitive surfaces of the bronchi are irradiated by these decays, the most energetic and destructive of which are the heavily ionizing, short range particles from the polonium isotopes ^{214}Po (E= 7.7 MeV) and ^{218}Po (E= 6.0 MeV) [Akeel and Hasan, 2003]

Most of the radon ingested with water is excreted through the urine over several days. There is some risk from drinking water with elevated radon, because radioactive decay can occur within the the body when tissues, such as the stomach lining, would be exposed. However, particles emitted by radon and its decay product in water prior to drinking quickly lose their energy and are taken up by other compounds in water, and do not themselves pose a health concern [EPA, 2005].

1.5 Rationale of the study

It is an established fact that high concentration of radon is carcinogenic. So one must be aware of his/her environs radon concentration and take the necessary steps for the reduction. It is also necessary to measure radon level of a given locale as part of accumulation of environmental radiation data. Future generations may use the data for possible nuclear activities.

In this regard, our country seem lagging behind even by African standards. Therefore this work can be regarded as the first serious attempt toward measurement and accumulation of base line data in environmental radiation. It can also serve as a pioneering work to continue further research in the area.

Chapter 2

Radon Measurement Methods

Many techniques have been developed over the years for measuring radon and radon progeny in air. Radon and radon progeny emit alpha and beta particles and gamma rays. Therefore, numerous techniques have been developed for measuring these radionuclides based on detecting alpha particles, beta particles, or gamma rays, independently or in some combination.

Radon measurement techniques are generally classified as *passive* and *active* methods. In the passive methods of measuring radon the measurement is usually made over a long period of time and the result is reported as the average over the measured time interval. In active measurement method, the radon concentration is measured at given measuring point in time.

In this chapter both methods are described and the different methods used for each category is discussed. These methods are standard methods which are described in detail in "indoor radon and radon decay product measurement device protocols" published by U.S. environmental protection agency [EPA, 1992].

2.1 Passive Measuring Methods

In this category of measurement methods; Solid state nuclear track detector(SSNTD), Activated charcoal(AC), Charcoal liquid scintillation(LS), and Electret ion chamber(EC) methods are the prominent ones.

2.1.1 Solid State Nuclear Track Detector

Solid State Nuclear Track Detector (SSNTD) consists of a small piece of plastic or film enclosed in a container. Radon diffuses into the container and particles emitted by the radon and its decay products strike the detector and produce submicroscopic damage tracks. At the end of the measurement period, the detectors are returned to the laboratory. Plastic detectors are placed in a caustic solution that accentuates the damaged tracks so they can be counted using an automated counting system. The number of tracks per unit area is correlated to the radon concentration in air. The number of tracks per unit of analyzed detector area produced per unit of time minus the background is proportional to the radon concentration.

SSNTD is mostly made up of detection material and detection chamber. The most popular member of SSNTDs family detection material is CR-39. It has good sensitivity, stability against various environmental factors, and high degree of optical clarity. The detector chamber is a cylindrical cup. Carbon is impregnated in the wall material, polypropylene, to enhance electrical conductivity and to avoid the problem of electrostatic charge. Radon enters the holder with a half-time for entry about 1 minute, which is short compared with the radon half-life of 3.82 days. This means that the radon concentration inside the detector chamber quickly approaches that of outside. It can be shown that the long-term average radon concentration inside the detector chamber is the same as that outside, despite any variations in the outside concentration. But the radon concentration may be overestimated because the short half-time for entry will allow some thoron to enter the detector [Ahn and Lee, 2005].

The optimal use of any track detector is largely dependent on standardization of various etching parameter. CR-39 samples are irradiated using an alpha source. Irradiated CR-39 samples can be etched in a solution. NaOH solution is most popular etchant and has been extensively studied. Varying concentrations of NaOH solutions can be used at different temperatures and periods. The etched tracks can be observed using an optical microscope. Calibration experiment can be carried out to evaluate the relationship between the track density recorded and the radon concentration. [Ahn and Lee, 2005]

2.1.2 Activated charcoal (AC)

In the last years, a lot of work has been done on the measurement of radon by adsorption on activated charcoal based on its well known property of adsorbing different gases and vapors, including radon. In most cases, the quantity of ^{222}Rn adsorbed is later measured by counting the gamma ray emissions of both ^{214}Pb and ^{214}Bi. This is possible due to the short half lives of these progeny.

ACs are passive devices requiring no power to function. The passive nature of the activated charcoal allows continual adsorption and the desorption of radon. During the measurement period, the adsorbed radon undergoes radioactive decay. Therefore, the technique does not integrate uniformly radon concentrations during the exposure period. As with all devices that store radon, the average concentration calculated using the mid-exposure time is subject to error if the ambient radon concentration varies substantially during the measurement period.

A device used most commonly consists of a circular container filled with activated charcoal. One side of the container is fitted with a screen that keeps the charcoal in but allows air to diffuse into the charcoal.

In some cases, the charcoal container has a diffusion barrier over the opening. For longer exposures, this barrier improves the uniformity of response to variations of radon concentration with time. Desiccant is also incorporated in some containers to reduce interference from moisture adsorption during longer exposures. Another variation of the charcoal container has charcoal packaged inside a sealed bag, allowing the radon to diffuse through the bag. All ACs are sealed with a radon-proof cover to outer container after preparation.

The measurement is initiated by removing the cover to allow radon-laden air to diffuse into the charcoal bed where the radon is adsorbed onto the charcoal. At the end of measurement period, the device is resealed securely and returned to laboratory for analysis.

At the laboratory, the ACs are analyzed for radon decay products by placing the charcoal, still in its container, directly on a gamma detector. Corrections may be needed to account for the the reduced sensitivity of the charcoal due to adsorbed water. This correction may be done by weighing each detector when it is prepared and then reweighing it when it is returned to the laboratory for analysis. Any

weight increase is attributed to water adsorbed on the charcoal. The weight of water gained is correlated to a correction factor. This conversion factor is used to correct the analytical results.

This correction is not needed if the configuration of the AC is modified to reduce significantly the adsorption of water and if the user has demonstrated experimentally that, over a wide range of humidities, there is negligible change in the collection efficiency of the charcoal within the specified exposure period.

The advantage of this technique is that it is completely passive, of very low cost, higher efficiency and a lower detection limit compared with gamma-spectrometry methods. This measurement method can be fully automated and is completely independent of humidity till 7 days of exposure.

2.1.3 Charcoal liquid scintillation (LS)

The frequently used type of LS device is a capped liquid scintillation vial which contains charcoal. In some cases, the vial contains a diffusion barrier over the charcoal which improves the uniformity of response of the device to variations of radon concentration with time, particularly for longer exposures. Some LS devices include a few grams of desiccant which reduces interference from moisture adsorption by the charcoal. All LS devices are sealed with a radon proof closure after preparation.

A measurement with LS device is initiated by removing the radon proof closure to allow radon-laden air to diffuse into the charcoal where the radon is adsorbed. At the end of the exposure (typically two to seven days), the device is resealed securely and returned to the laboratory for analysis.

At the laboratory, the devices are prepared for analysis by radon adsorption techniques. This technique transfers reproducibly a major fraction of the radon adsorbed on the charcoal into a vial of liquid scintillation fluid containing the dissolved radon are placed in a liquid scintillation counter and counted for a specified number of minutes (e.g. 10 minutes) or until the standard deviation of the count is acceptable (e.g., less than 10 percent)

2.1.4 Electret ion chamber (EC)

There are short-term and long-term ECs. They require no power, and function as true integrating detectors, measuring the average concentration during the measurement period.

The EC contains a charged electret (an electrostatically charged disk of Teflon) which collects ions formed in the chamber by radiation emitted from radon and radon decay products. When the device is exposed, radon diffuses into the chamber through filtered opening. Ions which are generated continually by the decay of radon and radon decay products are drawn to the surface of the electret and reduce its surface voltage. The amount of voltage reduction is related directly to the average radon concentration and the duration of exposure period. ECs can be deployed for exposure periods of two days to 12 months, depending upon the thickness of the electret and the volume of the ion chamber chosen for use. These deployment periods are flexible, and valid measurements can be made with other deployment periods depending on the application.

The electret must be removed from the EC chamber and the electret voltage measured with a special surface voltmeter both before and after exposure. To determine the average radon concentration during the exposure period, the difference between the initial and final voltages is divided first by a calibration factor and then by the number of exposure days. A background concentration equivalent of ambient gamma radiation is subtracted to compute radon concentration. Electret voltage measurements can be made in a laboratory or in the field.

2.2 Active Measuring Methods

Grab radon sampling method, Pump/collapsible bag method and Three-day integrating evacuated scintillation cells method are the prominent radon measurement methods in this category. Brief description of these methods is presented in this section.

2.2.1 Grab radon sampling

In this method three techniques which are frequently used. These are

Grab radon / scintillation cell (GS) method In this method sample is collected by pumping air through an activated charcoal. A sample of air is drawn into and sealed in a flask or cell that has zinc sulfide phosphor coating on its interior surfaces. One surface of the cell is fitted with a clear window that is put in contact with a photomultiplier tube to count scintillations resulting from alpha disintegrations from the air sample interacting with the zinc sulfide coating. The number of pulses is proportional to the radon concentration in the cell. The cell is counted about four hours after filling to allow the short-lived radon decay products to reach equilibrium with the radon. Correction factors are applied to the counting results to compensate for decay during the time between collection and counting and for the decay during counting if the counting time is long (> one hour). In a variation of this method, used in some portable instruments, air is pumped continuously through a flow-through-type scintillation cell for just a few minutes. Alpha particles resulting from the decay of radon gas and decay products are counted as the gas is swept through.

Grab radon/ activted charcoal (GC) method Air pumped through activated charcoal to collect the sample is used in this method. A charcoal-filled cartridge is placed into a sampler and air is pumped through the carbon cartridge. The pump with a charcoal cartridge is not flow dependent but must remain operational at the sampling location until the charcoal collects enough radon to be in equilibrium with the radon at the sampling collection. A sampling duration of one hour has been found to be optimal for most systems. The cartridge must be weighed prior to and after sampling in order to correct for the reduced sensitivity of the charcoal due to adsorbed water. The cartridges are analyzed by placing them on a sodium iodide gamma scintillation system or a germanium gamma detector.

Grab radon pump / collapsible bag (GB) method This method uses the same technology desribed in the pump / collapsible bag devices (PB) which will be discussed in the next subsection.The GB method discussed here differs only in that the bag is filled over a much shorter collection period than the PB.

Grab radon and thoron progeny sampling using Geiger-Muller counter

This is another method of grab sampling which is based on direct beta counting of filtered aerosol sample over successive time intervals by end-window Geiger-Müller counter. This method can be used for simultaneous measurement of radon and thoron decay products. The experiment which will be discussed in this paper was done using this method. So the method will be explained in detail in the next chapter.

2.2.2 Pump / collapsible bag (PB)

One of the older and simpler methods of making an integrated measurement of the concentration of radon over a period of time is to collect a sample of the ambient air in a radon-proof container over the desired sampling time period and measure the resulting radon concentration in the container.

One practical method is to use a small pump with a very low and uniform flow rate to pump ambient air into an inflatable and collapsible radon proof bag.

2.2.3 Three-day integrating evacuated scintillation cells (SC)

This method typically uses Lucas type scintillation cells that have been outfitted with a restricter valve attached to the main valve. Samples are collected by opening the valve on an evacuated cell. The restricter valve is set so that the cells fill from a 30-inch mercury (Hg) vacuum to about 80 percent of its capacity over a three day period. At the end of the measurement period, the valve is closed and returned to the analysis laboratory. Since the volume of the cell is known, the exact volume of filtered air collected over the three day measurement period can be calculated from the vacuum gauge reading at the end of the sampling period.

The sample is analyzed on an alpha scintillation counter. Prior to counting, the pressure in the cell is brought to one atmosphere by adding radon-free air so that the sample is analyzed under the same conditions that prevailed during calibration of the cell. To allow radon and progeny to grow into equilibrium and to allow any radon decay products that may have been collected to decay, the sample should be collected no sooner than four hours after the end of the measurement.

Chapter 3

Materials and Methods

3.1 Materials

The materials used for the experiment of radon decay products and thoron decay products measurement were

- Sampling head
- Glass fiber filter
- End-window GM tube
- Nuclear counter containing high voltage supply
- Air suction pump

To lower the limit of detection Papp [Papp, 1997] suggested to use glass fiber filter, high sampling flow rate and long duration of sampling. In this experiment also this suggestion was taken into consideration.

3.1.1 The sampling head

The design details of the sampling head are shown in figure 3.1. This design is the same as that used by Z. Papp etal. It was crafted by ANBO Engineering firm in Addis Ababa.

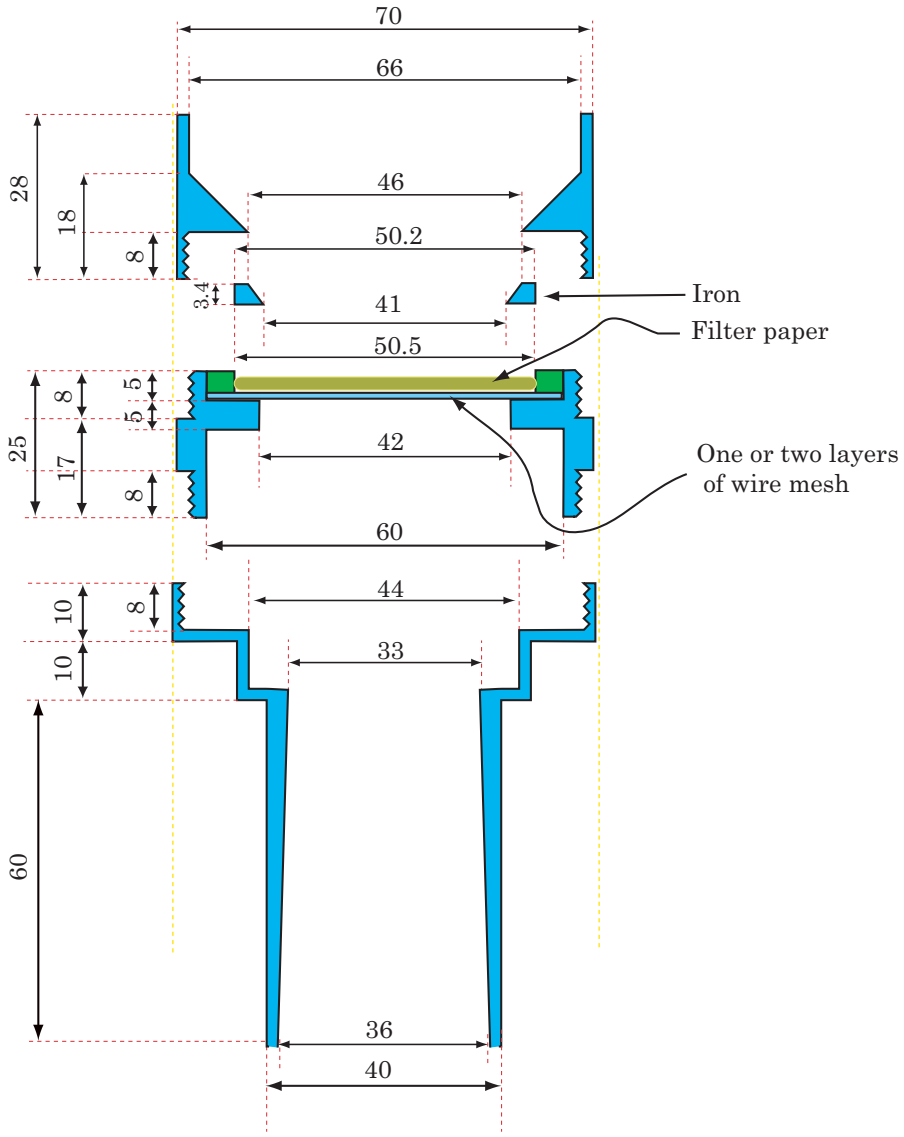

Figure 3.1: Air Sampling Head

3.1.2 Filtering air

Aerosol samples were collected on a glass fiber filter by drawing air through it. The filter used has a thickness of 0.0095 gcm^{-2} and dimensions of $2.9\,\mathrm{cm} \times 2.8\,\mathrm{cm}$. Aerosols were collected on a circular spot of 1.8 cm diameter. To pump air Genevao rotary piston vacuum pump was used. The air flow rate, during sampling, was 112 litres/min. A rubber tube connected the sampling head and the pump.

3.2 Methods

3.2.1 The counting process

For the counting process a GM tube with a nuclear counter was used. The GM counter has a window thickness of .002 g cm^{-2} and a diameter of 1.8 cm. The operating voltage the GM counter was determined to be 460 V.

Air was sampled on the filter for about 20 minutes at different times of the day (i.e morning, noon and evening). After a short time of the end of sampling (1 minute for most of the cases), the filter was placed below the GM tube. The distance between the tube and the filter was 9 mm. The total beta counts over a series of successive time intervals were recorded.

The background counting rate was also measured by using clean filter. It was found to be 47.9/min , 45.3/min and 42.3/min for morning , noon and evening times respectively.

3.2.2 Mathematical model

Activity concentration of airborne radon decay products and thoron decay products were determined by similar mathematical computations used by Raabe and Wrenn [Raabe and E.Wrenn, 1969] and Papp and Daróczy [Papp and Daróczy, 1997]

The computations proceed as follows

1. The differential equations which describe the collection and the decay during collection of the daughters are solved.

2. The differential equations which describe the decay of the daughters on the sample after collection is complete are solved.

3. A weighted least-squares regression analysis is performed to mathematically fit the observations of counts during various counting periods to the general decay equation for the sample. This provides the number of atoms of each daughter present on the sample at the end of collection period from which the number concentrations of the daughters in the atmosphere are calculated.

Let the numbers 1 to 7 represent ^{218}Po ,^{214}Pb and ^{214}Bi for radon decay products ; ^{212}Pb ^{212}Bi and ^{208}Tl for thoron decay products and U for unknown beta emitter with long half life respectively.

Constants:

K = Air sampling flow rate;
T = Air sampling time;
t_b = beginning of a counting time interval;
t_c = end of a counting time interval;
C = total beta counts measured over the time interval (t_b , t_c);
M = number of the counting time intervals ;
ϵ_i = beta counting efficiencies for the isotopes one by one (i = 2,3,...,7);
λ_i = decay constants , (i = 1,2,...,7) .

Variables :

n_i = numbers of atoms in a unit volume of the sampled air , (i = 1,2,...7);
a_i = activities of isotopes in a unit volume of the sampled air, (i = 1,2,...7) ;
N_i = numbers of atoms in the filter , (i = 1,2,...7) ;
N_{Ti} = numbers of atoms in the filter at the end of sampling , (i= 1,2,...,7);
t = time elapsed since the end of sampling (t = 0 at the end of sampling);
CR = total beta counting rate .

Assuming that k and n_i are constant during the sampling period the differential equations describing the buildup and decay of atoms on the sample are :

$$dN_1 = kn_1dt - \lambda_1 N_1 dt, \qquad N_1(0) = 0 \qquad \text{(3.1a)}$$

$$dN_2 = kn_2dt - \lambda_2 N_2 dt + \lambda_1 N_1 dt, \qquad N_2(0) = 0 \qquad \text{(3.1b)}$$

$$dN_3 = kn_3dt - \lambda_3 N_3 dt + \lambda_2 N_2 dt, \qquad N_3(0) = 0 \qquad \text{(3.1c)}$$

$$dN_4 = kn_4dt - \lambda_4 N_4 dt, \qquad N_4(0) = 0 \qquad \text{(3.1d)}$$

$$dN_5 = kn_5dt - \lambda_5 N_5 dt + \lambda_4 N_4 dt, \qquad N_5(0) = 0 \qquad \text{(3.1e)}$$

$$dN_6 = kn_6dt - \lambda_6 N_6 dt + \lambda_5 N_5 dt, \qquad N_6(0) = 0 \qquad \text{(3.1f)}$$

$$dN_7 = kn_7dt - \lambda_7 N_7 dt, \qquad N_7(0) = 0 \qquad \text{(3.1g)}$$

The solution for the buildup and decay equations shown in Equations 3.1 are given by Equations 3.2 as :

$$N_1 = kn_1\left[\frac{1-e^{-\lambda_1 t}}{\lambda_1}\right] \tag{3.2a}$$

$$N_2 = kn_1\left[\frac{1-e^{-\lambda_2 t}}{\lambda_2} - \frac{e^{-\lambda_2 t}-e^{-\lambda_1 t}}{\lambda_1-\lambda_2}\right] + kn_2\left[\frac{1-e^{-\lambda_2 t}}{\lambda_2}\right] \tag{3.2b}$$

$$\begin{aligned} N_3 = kn_1\left[\frac{1-e^{-\lambda_3 t}}{\lambda_3} - \frac{e^{-\lambda_2 t}-e^{-\lambda_3 t}}{\lambda_3-\lambda_2} - \frac{\lambda_2(e^{-\lambda_2 t}-e^{-\lambda_3 t})}{(\lambda_3-\lambda_2)(\lambda_1-\lambda_2)} + \frac{\lambda_2(e^{-\lambda_3 t}-e^{-\lambda_1 t}}{(\lambda_1-\lambda_3)(\lambda_1-\lambda_2)}\right] \\ + kn_2\left[\frac{1-e^{-\lambda_3 t}}{\lambda_3} - \frac{(e^{-\lambda_2 t}-e^{-\lambda_3 t})}{\lambda_3-\lambda_2}\right] + kn_3\left[\frac{1-e^{-\lambda_3 t}}{\lambda_3}\right] \end{aligned} \tag{3.2c}$$

$$N_4 = kn_4\left[\frac{1-e^{-\lambda_4 t}}{\lambda_4}\right] \tag{3.2d}$$

$$N_5 = kn_4\left[\frac{1-e^{-\lambda_5 t}}{\lambda_5} - \frac{e^{-\lambda_5 t}-e^{-\lambda_4 t}}{\lambda_4-\lambda_5}\right] + kn_5\left[\frac{1-e^{-\lambda_5 t}}{\lambda_5}\right] \tag{3.2e}$$

$$\begin{aligned} N_6 = kn_4\left[\frac{1-e^{-\lambda_6 t}}{\lambda_6} - \frac{e^{-\lambda_5 t}-e^{-\lambda_6 t}}{\lambda_6-\lambda_5} - \frac{\lambda_5(e^{-\lambda_5 t}-e^{-\lambda_6 t})}{(\lambda_6-\lambda_5)(\lambda_5-\lambda_6)} + \frac{\lambda_5(e^{-\lambda_6 t}-e^{-\lambda_4 t})}{(\lambda_4-\lambda_6)(\lambda_4-\lambda_5)}\right] \\ + kn_5\left[\frac{1-e^{-\lambda_6 t}}{\lambda_6} - \frac{e^{-\lambda_5 t}-e^{-\lambda_6 t}}{\lambda_6-\lambda_5}\right] + kn_6\left[\frac{1-e^{-\lambda_6 t}}{\lambda_6}\right] \end{aligned} \tag{3.2f}$$

$$N_7 = kn_6\left[\frac{1-e^{-\lambda_7 t}}{\lambda_6}\right] \tag{3.2g}$$

$N_{Ti}(i = 1, 2, ..., 7)$, which is number of atom in the filter at the end of sampling can be expressed by replacing t by T, because end of sampling time is equal to the air sampling time (T). So $N_{Ti}(i = 1, 2, ..., 7)$ can be expressed as:

$$N_{T1} = kn_1\left[\frac{1-e^{-\lambda_1 T}}{\lambda_1}\right] \tag{3.3a}$$

$$N_{T2} = kn_1\left[\frac{1-e^{-\lambda_2 T}}{\lambda_2} - \frac{e^{-\lambda_2 T}-e^{-\lambda_1 T}}{\lambda_1-\lambda_2}\right] + kn_2\left[\frac{1-e^{-\lambda_2 T}}{\lambda_2}\right] \tag{3.3b}$$

$$\begin{aligned} N_{T3} = kn_1\left[\frac{1-e^{-\lambda_3 T}}{\lambda_3} - \frac{e^{-\lambda_2 T}-e^{-\lambda_3 T}}{\lambda_3-\lambda_2} - \frac{\lambda_2(e^{-\lambda_2 T}-e^{-\lambda_3 T})}{(\lambda_3-\lambda_2)(\lambda_1-\lambda_2)} + \frac{\lambda_2(e^{-\lambda_3 T}-e^{-\lambda_1 T})}{(\lambda_1-\lambda_3)(\lambda_1-\lambda_2)}\right] \\ + kn_2\left[\frac{1-e^{-\lambda_3 T}}{\lambda_3} - \frac{(e^{-\lambda_2 T}-e^{-\lambda_3 T})}{\lambda_3-\lambda_2}\right] + kn_3\left[\frac{1-e^{-\lambda_3 T}}{\lambda_3}\right] \end{aligned} \tag{3.3c}$$

$$N_{T4} = kn_4\left[\frac{1-e^{-\lambda_4 T}}{\lambda_4}\right] \tag{3.3d}$$

$$N_{T5} = kn_4\left[\frac{1-e^{-\lambda_5 T}}{\lambda_5} - \frac{e^{-\lambda_5 T}-e^{-\lambda_4 T}}{\lambda_4-\lambda_5}\right] + kn_5\left[\frac{1-e^{-\lambda_5 T}}{\lambda_5}\right] \tag{3.3e}$$

$$N_{T6} = kn_4\left[\frac{1-e^{-\lambda_6 T}}{\lambda_6} - \frac{e^{-\lambda_5 T}-e^{-\lambda_6 T}}{\lambda_6-\lambda_5} - \frac{\lambda_5(e^{-\lambda_5 T}-e^{-\lambda_6 T})}{(\lambda_6-\lambda_5)(\lambda_5-\lambda_6)} + \frac{\lambda_5(e^{-\lambda_6 T}-e^{-\lambda_4 T})}{(\lambda_4-\lambda_6)(\lambda_4-\lambda_5)}\right] + kn_5\left[\frac{1-e^{-\lambda_6 T}}{\lambda_6} - \frac{e^{-\lambda_5 T}-e^{-\lambda_6 T}}{\lambda_6-\lambda_5}\right] + kn_6\left[\frac{1-e^{-\lambda_6 T}}{\lambda_6}\right] \quad (3.3f)$$

$$N_{T7} = kn_6\left[\frac{1-e^{-\lambda_7 T}}{\lambda_6}\right] \quad (3.3g)$$

$n_i(i = 1, 2, ..., 7)$ can be expressed from equations (3.3a) to (3.3g) as follows

$$n_1 = \frac{\lambda_1 N_{T1}}{k(1-e^{-\lambda_1 T})} \quad (3.4a)$$

$$n_2 = \frac{\lambda_2 N_{T2}}{k(1-e^{-\lambda_2 T})} - n_1\left[1 - \frac{\lambda_2(e^{-\lambda_2 T}-e^{-\lambda_1 T})}{(\lambda_1-\lambda_2)(1-e^{-\lambda_2 T})}\right] \quad (3.4b)$$

$$n_3 = \frac{\lambda_3 N_{T3}}{k(1-e^{-\lambda_3 T})} - n_2\left[1 - \frac{\lambda_3(e^{-\lambda_2 T}-e^{-\lambda_3 T})}{(\lambda_3-\lambda_2)(1-e^{-\lambda_3 T})}\right] - n_1\left[1 - \frac{\lambda_3(e^{-\lambda_2 T}-e^{-\lambda_3 T})}{(\lambda_3-\lambda_2)(1-e^{-\lambda_3 T})} - \frac{\lambda_2\lambda_3(e^{-\lambda_2 T}-e^{-\lambda_3 T})}{(\lambda_3-\lambda_2)(\lambda_1-\lambda_2)(1-e^{-\lambda_3 T})} + \frac{\lambda_2\lambda_3(e^{\lambda_3 T}-e^{-\lambda_1 T})}{(\lambda_1-\lambda_3)(\lambda_1-\lambda_2)(1-e^{-\lambda_3 T})}\right] \quad (3.4c)$$

$$n_4 = \frac{\lambda_4 N_{T4}}{k(1-e^{-\lambda_4 T})} \quad (3.4d)$$

$$n_5 = \frac{\lambda_5 N_{T5}}{k(1-e^{-\lambda_5 T})} - n_4\left[1 - \frac{\lambda_5(e^{-\lambda_5 T}-e^{-\lambda_4 T})}{(\lambda_4-\lambda_5)(1-e^{-\lambda_5 T})}\right] \quad (3.4e)$$

$$n_6 = \frac{\lambda_6 N_{T6}}{k(1-e^{-\lambda_6 T})} - 0.36n_5\left[1 - \frac{\lambda_6(e^{-\lambda_5 T}-e^{-\lambda_6 T})}{(\lambda_6-\lambda_5)(1-e^{-\lambda_6 T})}\right] - 0.36n_4\left[1 - \frac{\lambda_6(e^{-\lambda_5 T}-e^{-\lambda_6 T})}{(\lambda_6-\lambda_5)(1-e^{-\lambda_6 T})} - \frac{\lambda_5\lambda_6(e^{-\lambda_5 T}-e^{-\lambda_6 T})}{(\lambda_6-\lambda_5)(\lambda_4-\lambda_5)(1-e^{-\lambda_6 T})} + \frac{\lambda_5\lambda_6(e^{-\lambda_6 T}-e^{-\lambda_4 T})}{(\lambda_4-\lambda_6)(\lambda_4-\lambda_5)(1-e^{-\lambda_6 T})}\right] \quad (3.4f)$$

$$n_7 = \frac{\lambda_7 N_{T7}}{k(1-e^{-\lambda_7 T})} \quad (3.4g)$$

The solutions of the equation for the decay after the end of sampling are:

$$N_1 = N_{T1}e^{-\lambda_1 t} \tag{3.5a}$$

$$N_2 = N_{T1}\left[\lambda_1 \frac{e^{-\lambda_2 t} - e^{-\lambda_1 t}}{\lambda_1 - \lambda_2}\right] + N_{T2}e^{-\lambda_2 t} \tag{3.5b}$$

$$N_3 = N_{T1}\left[\frac{}{\lambda_1\lambda_2(e^{-\lambda_2 t} - e^{-\lambda_3 t})}(\lambda_3 - \lambda_2)(\lambda_1 - \lambda_2) - \frac{\lambda_1\lambda_2(e^{-\lambda_3 t} - e^{-\lambda_1 t})}{(\lambda_1 - \lambda_3)(\lambda_1 - \lambda_2)}\right] + N_{T2}\left[\frac{\lambda_2(e^{-\lambda_2 t} - e^{-\lambda_3 t}}{\lambda_3 - \lambda_2}\right] + N_{T3}e^{-\lambda_3 t} \tag{3.5c}$$

$$N_4 = N_{T4}e^{-\lambda_4 t} \tag{3.5d}$$

$$N_5 = N_{T4}\left[\frac{\lambda_4(e^{-\lambda_5 t} - e^{-\lambda_4 t}}{\lambda_4 - \lambda_5}\right] + N_{T5}e^{-\lambda_5 t} \tag{3.5e}$$

$$N_6 = 0.36N_{T4}\left[\frac{\lambda_4\lambda_5(e^{-\lambda_5 t} - e^{-\lambda_6 t})}{(\lambda_6 - \lambda_5)(\lambda_4 - \lambda_5)} - \frac{\lambda_4\lambda_5(e^{-\lambda_6 t} - e^{-\lambda_4 t})}{(\lambda_4 - \lambda_6)(\lambda_4 - \lambda_5)}\right] + .36N_{T5}\left[\frac{\lambda_5(e^{-\lambda_5 t} - e^{-\lambda_6 t}}{\lambda_6 - \lambda_5}\right] + N_{T6}e^{-\lambda_6 t} \tag{3.5f}$$

$$N_7 = N_{T7}e^{-\lambda_7 t} \tag{3.5g}$$

The count rate (CR) can be described by the equation

$$CR = \sum_{i=2}^{7} \epsilon_i \lambda_i N_i \tag{3.6}$$

in the above equation ^{218}Po is not considered because it is mostly alpha emitter.

Replacing N_i by substituting (3.5a) to (3.5g) and integrating with respect to t between t_b and t_c, it follows

$$C = \sum_{i=1}^{7} N_{Ti} X_i \tag{3.7}$$

where

$$X_1 = \frac{\epsilon_2\lambda_2(e^{-\lambda_1 b} - e^{-\lambda_1 c})}{\lambda_2 - \lambda_1} - \frac{\epsilon_2\lambda_1(e^{-\lambda_2 b} - e^{-\lambda_2 c})}{\lambda_2 - \lambda_1} + \frac{\epsilon_3\lambda_2\lambda_3(e^{-\lambda_1 b} - e^{-\lambda_1 c})}{(\lambda_2 - \lambda_1)(\lambda_3 - \lambda_1)}$$
$$- \frac{\epsilon_3\lambda_1\lambda_3(e^{-\lambda_2 b} - e^{-\lambda_2 c})}{(\lambda_2 - \lambda_1)(\lambda_3 - \lambda_2)} + \frac{\epsilon_3\lambda_1\lambda_2(e^{-\lambda_3 b} - e^{-\lambda_3 c})}{(\lambda_3 - \lambda_2)(\lambda_3 - \lambda_1)} \tag{3.8a}$$

$$X_2 = \epsilon_2(e^{-\lambda_2 b} - e^{-\lambda_2 c}) + \frac{\epsilon_3\lambda_3(e^{-\lambda_2 b} - e^{-\lambda_2 c})}{\lambda_3 - \lambda_2} - \frac{\epsilon_3\lambda_2(e^{-\lambda_3 b} - e^{-\lambda_3 c})}{(\lambda_3 - \lambda_2)} \tag{3.8b}$$

$$X_3 = \epsilon_3(e^{-\lambda_3 b} - e^{-\lambda_3 c}) \tag{3.8c}$$

$$X_4 = \epsilon_4(e^{-\lambda_4 b} - e^{-\lambda_4 c}) + \frac{\epsilon_5\lambda_5(e^{-\lambda_4 b} - e^{-\lambda_4 c})}{\lambda_5 - \lambda_4} - \frac{\epsilon_5\lambda_4(e^{-\lambda_5 b} - e^{-\lambda_5 c})}{(\lambda_5 - \lambda_4)}$$
$$+ \frac{0.36\epsilon_6\lambda_5\lambda_6(e^{-\lambda_4 b} - e^{-\lambda_4 c})}{(\lambda_5 - \lambda_4)(\lambda_6 - \lambda_4)} - \frac{0.36\epsilon_6\lambda_4\lambda_6(e^{-\lambda_5 b} - e^{-\lambda_5 c})}{(\lambda_5 - \lambda_4)(\lambda_6 - \lambda_5)} + \frac{0.36\epsilon_6\lambda_4\lambda_5(e^{-\lambda_6 b} - e^{-\lambda_6 c})}{(\lambda_6 - \lambda_5)(\lambda_6 - \lambda_4)} \tag{3.8d}$$

$$X_5 = \epsilon_5(e^{-\lambda_5 b} - e^{-\lambda_5 c}) + \frac{0.36\epsilon_6\lambda_6(e^{-\lambda_5 b} - e^{-\lambda_5 c})}{(\lambda_6 - \lambda_5)} - \frac{0.36\epsilon_6\lambda_5(e^{-\lambda_6 b} - e^{-\lambda_6 c})}{(\lambda_6 - \lambda_5)} \tag{3.8e}$$

$$X_6 = \epsilon_6(e^{-\lambda_6 b} - e^{-\lambda_6 c}) \tag{3.8f}$$

$$X_7 = \epsilon_7(e^{-\lambda_7 b} - e^{-\lambda_7 c}) \tag{3.8g}$$

Assume that the total beta counts were measured over M successive time intervals. This series of measurements can be described by a series of linear equations as

$$C_m = \sum_{i=1}^{7} N_{Ti} X_{mi}, (m = 1, 2, ..., M) \tag{3.9}$$

C_m are the measured total beta counts ,and X_{mi} are the values of X_i for different time intervals , respectively.

N_{Ti} could be estimated from (3.9) using the least square fitting method. n_i could be computed according to (3.4a) to (3.4g).

From these concentrations the Equivalent Equilibrium Concentration (EEC) of ^{222}Rn and ^{220}Rn can be obtained. EEC can be given interms of the individual decay product concentrations of ^{222}Rn and ^{220}Rn as

$$EEC_{Rn} = 0.105\, C_1 + .515\, C_2 + 0.380\, C_3$$

where C_1, C_2, and C_3 represent concentrations of ^{218}Po, ^{214}Pb and ^{214}Bi respectively.

$$EEC_{Th} = 0.913\,C_1 + 0.087\,C_2$$

where C_1, C_2 represent ^{212}Pb and ^{212}Bi respectively.

The Defined solid angle absolute beta counting (DSAABC) method was used to determine the counting efficiencies ϵ_is in (3.8a) to (3.8g), one by one. This method will be explained briefly in the next section.

3.2.3 Defined Solid Angle Absolute Beta Counting Method

Introduction

Defined solid angle absolute β-counting (DSAABC) is one of the oldest methods for the determination of the activity of β-emitting radionuculides. It was developed nearly 60 years ago by authors like B.P.Burtt [Burtt, 1949] and others.

This method mostly concerns on the idea that the counting rate of a beta emitter relative to the activity rate depends upon the geometry, the percent of solid angle about the source subtended by the sensitive volume of the counter, and absorption of the radiations by the air and window of the counter and scattering from the source support and assembly.

So the counting efficiencies for the radon decay products and thoron decay products can be evaluated one by one using the defined solid angle absolute beta counting (DSAABC).

However, several problems may arise if someone wants to apply this method in the field of environmental radioanalysis. The most difficult one is that the counting rate is influenced by numerous effects which have to be precisely considered if accurate activity results are needed.

It is often said that it is not worth the trouble to deal with the problems of this method because

1. High accuracy cannot be reached
2. β emitters cannot be easily identified
3. relative counting using certified reference samples is simpler and more accurate
4. more suitable methods are available

The first of the above arguments is indisputable but high accuracy is not necessarily needed in all fields of environmental radioanalysis. As to the second argument, identification of the emitters are exactly known. It has to be emphasized that relative counting as against absolute one may be more accurate only if the reference sample contains the same radionuclide(s) and has exactly the same dimensions, elemental composition and inner distribution of activity as those of the sample to be measured. The complete fulfilment of the above requirements is not easy in most cases, so the relative method may be either simpler or more accurate than the absolute one, but seldom may be both at the same time. It is true that modern methods for the detection of β particles or γ-rays, such as liquid scintillation counting (LSC) or semiconductor γ-spectrometry, are better choices in most cases. But there are special cases when the DSAABC method using an end-window Geiger-Müller (GM) can compete with the above methods or may be even more suitable. Samples have to be liquefied and in most cases also some chemical separations are needed for LSC. Semiconductor γ- spectrometers have low efficiency and cannot be used for the determination of of pure β-emitters. If, for example, low activities, have to be measured or the chemical treatment of the sample should be avoided for some reason then the DSAABC method is a cheap and technically simple one. [Papp, 1997]

Counting efficiency determination

Assume that the β-radiation of a thin sample containing one β-emitting radionuclide is measured by an end-window GM counter through a thin absorber in a fixed geometry. The nuclide has n different β-transitions with energies, $E_{\beta i}$ and intensities, $I_{\beta i}$ (i= 1,2,...,n ; $\sum_{i=1}^{n} I_{\beta i} \leq 1$), emits conversion electrons with p different energies, E_{cj} and intensities, I_{cj} (j=1,2,...,p) and γ-quanta and X-rays with q different energies, $E_{\gamma k}$ and intensities, $I_{\gamma k}$ (k= 1,2,...,q). According to Papp [Papp, 1997], the counting rate, CR, is related to the activity A, by

$$CR = A f_m f_c f_g \left[f_{se} \left(\sum_{i=1}^{n} I_{\beta i} f_{Wi} f_{Si} f_{Ai} f_{Bi} f_{Hi} + \sum_{j=1}^{p} I_{cj} f_{Ccj} f_{acj} \right) + \sum_{k=1}^{q} I_{\gamma k} f_{c\gamma k} f_{s\gamma k} f_{a\gamma k} \right] \tag{3.10}$$

where

f_m is for multiple counting

f_c is for loss due to random coincidence

f_g is for the solid angle geometry

f_{se} is for the intrinsic sensitivity of the counter for electrons

f_{Wi} are for the absorption of β-particles by the window and further absorbers

f_{Si} are for the effect of the sample in scattering and absorption of β-particles

f_{Ai} are for air scattering

f_{Bi} are for backscattering

f_{Hi} are for the effect of the housing in scattering β-particles into the counter

f_{Ccj} are for the true coincidences of conversion electrons with β-particles

f_{acj} are for the absorption of conversion electrons

$f_{c\gamma k}$ are for the true coincidences of γ-quanta and X-rays with β-particles and conversion electrons

$f_{s\gamma k}$ are for the intrinsic sensitivity of the detector for γ-quanta and X-rays

$f_{a\gamma k}$ are for the absorption of γ-quanta and X-rays

A can be determined from CR if the correction factors in (3.10) are measured, computed, estimated or eliminated in some way. Errors are introduced in this way into the final activity result. So it is recommended to choose the detector, the counting geometry and the structural materials like that the values of the factors be as near unity and their errors be as low as possible. The counting efficiency ϵ can be computed as $\epsilon = CR/A$.

In the discussion to determine the factors one by one papp [Papp, 1997], tried to attain the highest accuracy obtainable with reasonable effort. The less important factors and the errors of the evaluations have not been examined intensively.

$f_{se}\ and\ f_m$ are assumed to be close to unity for good GM tubes if the high voltage is chosen at the beginning of the plateau.

$f_A\ and\ f_H$ are close to unity if small sample-detector distance and spacious housing covered from inside by low atomic number material are used.

f_{Ccj} is equal to the probability of not detecting β-particle emitted simultaneously with the conversion electron. It can be estimated by the formula

$$f_{Ccj} = 1 - f_g(I_{\beta i} f_{Wi} f_{Si} f_{Bi}) \tag{3.11}$$

f_{acj} can be estimated using experimental data on the transmission of monoenenergetic electron beams.

$f_{s\gamma}$ can be measured by using ^{54}Mn and ^{57}Co reference point sources and by analyzing the γ-background in absorption curves measured by ^{134}Cs and ^{137}Cs point sources.

$f_{c\gamma k}$ can be estimated as

$$f_{C\gamma k} = 1 - f_g(I_{\beta i} f_{Wi} f_{Si} f_{Bi} + I_{cj} f_{Ccj} f_{acj}) \tag{3.12}$$

where i and j are the indexes of the corresponding β transition and conversion electron.

$f_{a\gamma}$ differs from unity only for X-rays. It can be estimated as

$$f_{a\gamma} = \exp(-\mu_\gamma W)$$

where W is the total thickness of the absorbers (detector window, air, added absorber) and μ_γ is the mass absorption coefficient which can be evaluated from literatures.

f_c becomes an important factor only in case of high values of CR (above 100-200 sec^{-1}). It can be computed for GM counters as $f_c = 1 - CR\tau$, where τ is the resolving time of the counter

f_g can be determined from the solid angle subtended by a circular aperture of radius R at a circular source of radius r, coaxial with the aperture, the distance of which from the aperture is equal to Z, in case of $r < R$ which is

$$G = \frac{1}{2}\left[1 - \frac{Z}{D}\right] - \frac{3r^2R^2Z}{16D^5} + \frac{5r^4R^2Z}{32D^9}\left[Z^2 - \frac{3}{4}R^2\right] - \frac{35r^6R^2Z}{256D^{13}\left[Z^4 - \frac{5}{2}R^2Z^2 + \frac{5}{8}R^4\right]} \tag{3.13}$$

where $D = (Z^2 + R^2)^{1/2}$ if R and Z are equal to the radius of the sensitive volume of the detector and the distance from the sample to the bottom surface of the sensitive volume, respectively. It can be assumed that the sensitive volume is cylindrical and its diameter is equal to that of the window.

f_W can be evaluated by the expression

$$f_W = \exp(-\mu_a W)$$

where μ_a is the mass-absorption coefficient and W is the summed thickness of the absorbers(window, absorber sheet and air) μ_a in function of E_β can be determined experimentally from the results of absorption measurements.

f_s is the most difficult factor that has complex character. It is reasonable to treat the different effects contributing in f_s separately. They are: self-absorption (f_{sa}), self-scattering (f_{ss}) and internal backscattering (f_{ib}). Thus f_s is written as the product of three factors, which are for the above effects:

$$f_s = f_{sa} f_{ss} f_{ib}$$

f_{ss} is close to unity if

1. near 2π-type geometry is used;
2. sample is made from low Z material;
3. most of the activity is on or close to the upper surface of the sample

f_{sa} = $[1 - \exp(-\mu_s d)]/(\mu_s d)$, where μ_s is the self absorption coefficient and d is the thickness of the sample.

f_{ib} is generally a phenomenon of second order but it becomes more significant in case of strongly decreasing exponential activity distribution.

using this method efficiencies 0.14313, 0.123516, 0.11697, 0.0774 and 0.1319 were obtained for ^{214}Pb, ^{214}Bi, ^{212}Pb, ^{212}Bi, ^{208}Tl respectively.

Chapter 4

Data Analysis and Discussion

4.1 Results

Measurements were taken in the nuclear physics laboratory located on the first floor of physics building. Air was sampled three times a day: Morning, Noon and Evening i.e. 7:00 to 8:00 A.M.; 1:00 to 2:00 P.M. and 6:00 to 7:00 P.M. respectively.

A total of 46 measurements were made and each was recorded for more than 7 hrs in successively increasing intervals of time. A typical measurement procedure is indicated in table 4.1. The first and the second columns in table 4.1 were recorded from the Geiger counter apparatus. The third term indicates the serial of the intervals of measurement and the fourth and the fifth columns indicate the beginning and end of diurnal time for the corresponding interval. The sixth column indicates time as measured from the end of sampling as origin. i.e. the time in the six column thus indicate the age of the filtered air sample as measured from the end of sampling. The seventh column shows the length of measurement of each time interval whereas the eighth column is the gross count in the interval.

The age of the filter, the length of the measuring time interval and the gross count obtained were fed in a computer programme, that computes the concentration of progeny and the equilibrium equivalent concentration for the two isotopes, from the observed decline in the observed count rates.

Table 4.1: Measurement Procedure in DSAABC Method

observe t	disply cnt	m	t_b	t_e	t (min)	Δt	count	Count rate
8:18:00	0	1	8:18:00	8:19:00	1	1	1760	1760
8:19:00	1760	2	8:19:00	8:20:00	2	1	1680	1680
8:20:00	3440	3	8:20:00	8:21:00	3	1	1640	1640
8:21:00	5080	4	8:21:00	8:22:00	4	1	1720	1720
8:22:00	6800	5	8:22:00	8:23:00	5	1	1660	1660
8:23:00	8460	6	8:23:00	8:24:00	6	1	1650	1650
8:24:00	10110	7	8:24:00	8:25:00	7	1	1600	1600
8:25:00	11710	8	8:25:00	8:26:00	8	1	1590	1590
8:26:00	13300	9	8:26:00	8:27:00	9	1	1580	1580
8:27:00	14880	10	8:27:00	8:28:00	10	1	1540	1540
8:28:00	16420	11	8:28:00	8:29:00	11	1	1560	1560
8:29:00	17980	12	8:29:00	8:30:00	12	1	1550	1550
8:30:00	19530	13	8:30:00	8:31:00	13	1	1550	1550
8:31:00	21080	14	8:31:00	8:32:00	14	1	1480	1480
8:32:00	22560	15	8:32:00	8:33:00	15	1	1490	1490
8:33:00	24050	16	8:33:00	8:35:00	16	2	2760	1380
8:35:00	26810	17	8:35:00	8:37:00	18	2	2810	1405
8:37:00	29620	18	8:37:00	8:39:00	20	2	2670	1335
8:39:00	32290	19	8:39:00	8:41:00	22	2	2630	1315
8:41:00	34920	20	8:41:00	8:43:00	24	2	2660	1330
8:43:00	37580	21	8:43:00	8:45:00	26	2	2430	1215
8:45:00	40010	22	8:45:00	8:47:00	28	2	2440	1220
8:47:00	42450	23	8:47:00	8:49:00	30	2	2360	1180
8:49:00	44810	24	8:49:00	8:51:00	32	2	2140	1070
8:51:00	46950	25	8:51:00	8:53:00	34	2	2180	1090
8:53:00	49130	26	8:53:00	8:55:00	36	2	2160	1080
8:55:00	51290	27	8:55:00	8:57:00	38	2	2130	1065
8:57:00	53420	28	8:57:00	8:59:00	40	2	2010	1005
8:59:00	55430	29	8:59:00	9:01:00	42	2	2020	1010
9:01:00	57450	30	9:01:00	9:03:00	44	2	1970	985
9:03:00	59420	31	9:03:00	9:06:00	46	3	2830	943
9:06:00	62250	32	9:06:00	9:09:00	49	3	2750	917
9:09:00	65000	33	9:09:00	9:12:00	52	3	2640	880
9:12:00	67640	34	9:12:00	9:15:00	55	3	2410	803
9:15:00	70050	35	9:15:00	9:18:00	58	3	2390	797
9:18:00	72440	36	9:18:00	9:21:00	61	3	2290	763
9:21:00	74730	37	9:21:00	9:24:00	64	3	2220	740
9:24:00	76950	38	9:24:00	9:27:00	67	3	2110	703
9:27:00	79060	39	9:27:00	9:30:00	70	3	2010	670
9:30:00	81070	40	9:30:00	9:33:00	73	3	1870	623
9:33:00	82940	41	9:33:00	9:36:00	76	3	1970	657
9:36:00	84910	42	9:36:00	9:39:00	79	3	1740	580
9:39:00	86650	43	9:39:00	9:42:00	82	3	1680	560
9:42:00	88330	44	9:42:00	9:45:00	85	3	1630	543
9:45:00	89960	45	9:45:00	9:48:00	88	3	1710	570
9:48:00	91670	46	11:30:00	11:34:00	193	4	1020	255
11:30:00	0	47	11:34:00	11:38:00	197	4	910	228
11:34:00	1020	48	11:38:00	11:42:00	201	4	1010	253
11:38:00	1930	49	11:42:00	11:46:00	205	4	1030	258
11:42:00	2940	50	11:46:00	11:50:00	209	4	970	243
11:46:00	3970	51	17:07:00	17:11:00	530	4	650	163
11:50:00	4940	52	17:11:00	17:15:00	534	4	680	170
17:07:00	0	53	17:15:00	17:19:00	538	4	770	193
17:11:00	650	54	17:19:00	17:23:00	542	4	740	185
17:15:00	1330	55	17:23:00	17:27:00	546	4	710	178
17:19:00	2100	56						
17:23:00	2840	57						
17:27:00	3550	58						
17:31:00								

4.2 Analysis

In the computation the program assumes the following points

- The assumption of the existence of longlived β- emitter in the sampled air has resulted in mathematically correct but physically meaningless concentrations that fit to the observed gross count. Thus the concentration of longlived β-emitter was assumed to be zero.
- The daughter products of ^{222}Rn vis ^{218}Po ($t_{1/2} = 3.05$ min) and ^{214}Pb ($t_{1/2} = 26.8$ min) are linked together by the ratio

$$\frac{\text{Activity concentration of } ^{214}\text{Pb}}{\text{Activity concentration of } ^{218}\text{Po}} = 0.5$$

- The daughter products of ^{220}Rn namely ^{212}Bi ($t_{\frac{1}{2}} = 61$ min) and ^{208}Tl ($t_{\frac{1}{2}} = 3$ min) are linked together when the graph is plotted. This stems from the fact that the activities of these two isotopes are very small as compared to that of ^{222}Rn daughters.

From the plot using the program the following results was observed

- Activities of isotopes in a unit volume of sampled air
- Standard deviation which can be regarded as random error
- The beta count rate measured over the time interval specified for all the counting intervals as a function of time
- Contribution of the individual decay products for all the counting intervals, as a function of time.
- Sum of the individual contributions for some counting intervals
- The Equilibrium Equivalent Concentration (EEC) of ^{222}Rn and ^{220}Rn

Based on the data of table 4.1 the results observed is shown in figure 4.1.

Using the same procedure the computation was done for the rest of the datas. The computed activities of Radon daughters and the equilibrium equivalent concentration of the two radon isotopes is shown in table 4.2.

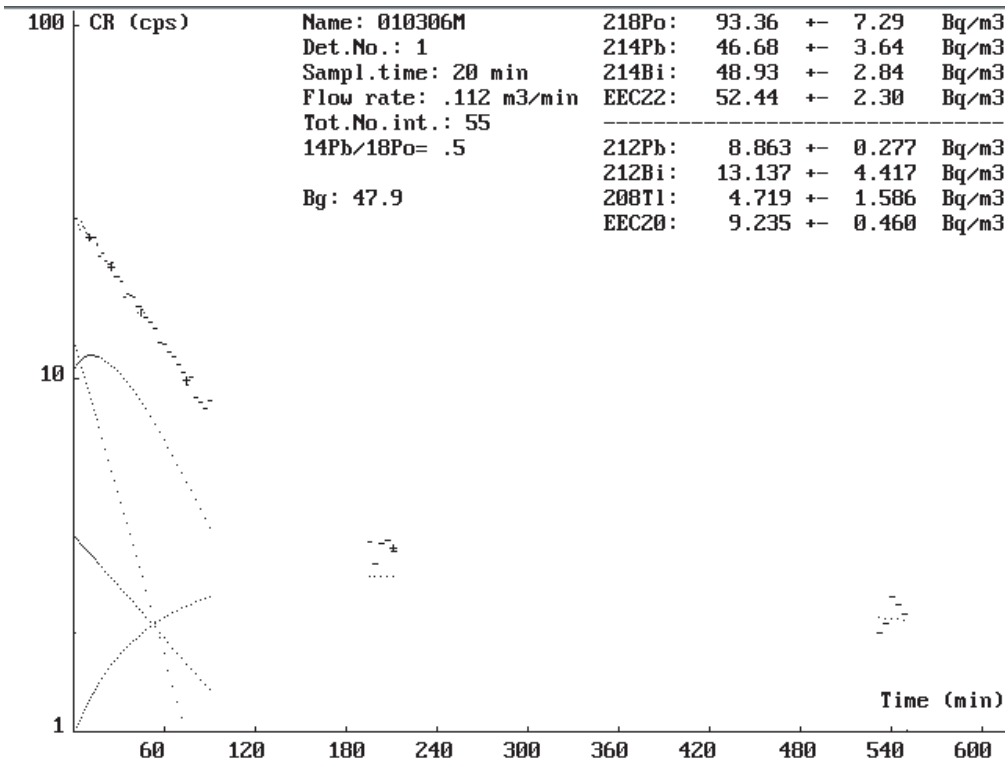

Figure 4.1: Concentration of daughters determined from gross β count

The naming of the experiment consists of six digits, ie the first two digit stand or the code of the placing measurement. The second two digits represent the date and the last two represent the month and the last letter represents time of the day i.e. (M for morning. N for noon for noon and E for evening)

Table 4.2: Computed activity concentration of Radon Progeny and Equilibrium Activity Concentrations

Sample code	218Po	214Pb	214Bi	EEC_{222}	212Pb	212Bi	208Tl	EEC_{220}	Remark
012005E	20.77 ± 0.87	10.39 ± 0.43	7.75 ± 0.96	10.48 ± 0.44	3.723± 0.076	3.35± 0.068	1.203 ± 0.024	3.69 ± 0.069	
012005M	75.25 ± 2.04	37.63 ± 1.02	35.02 ± 2.49	40.59 ± 1.1	6.893± 0.138	6.203± 0.124	2.228 ± 0.045	6.833 ± 0.127	
012005N	12.89 ± 0.79	6.44 ± 0.4	2.15 ± 0.87	5.49 ± 0.4	2.317± 0.065	2.085± 0.059	0.749 ± 0.021	2.297 ± 0.06	
012105E	67.67 ± 4.25	33.84 ± 2.13	31.55 ± 2.02	36.52 ± 1.41	8.249± 0.254	7.459± 2.63	2.679 ± 0.975	8.18 ± 0.326	
012105M	19.42 ± 0.72	9.71 ± 0.36	4.65 ± 0.81	8.81 ± 0.37	1.931± 0.06	1.738± 0.054	0.624 ± 0.019	1.915 ± 0.055	
012105N	23.75 ± 2.21	11.87 ± 1.11	8.32 ± 2.48	11.78 ± 1.12	4.272± 0.188	3.845± 0.169	1.381 ± 0.061	4.235 ± 0.172	
012205M	125.64 ± 5.44	62.82 ± 2.72	53.64 ± 6.13	65.94 ± 2.77	10.55± 0.45	9.497± 0.405	3.411 ± 0.145	10.46 ± 0.412	
012405E	28.65 ± 3.06	14.33 ± 1.53	12.72 ± 1.41	15.22 ± 1.01	4.272± 0.205	8.673± 1.979	3.115 ± 0.711	4.655 ± 0.254	
012405M	149.77 ± 3.05	74.89 ± 1.52	70.73 ± 3.49	81.17 ± 1.57	14.37± 0.238	12.93± 0.214	4.645 ± 0.077	14.24 ± 0.218	
012505E	64.4 ± 4.16	32.2 ± 2.08	31.02 ± 1.98	35.13 ± 1.38	7.914± 0.247	10.2± 2.566	3.662 ± 0.922	8.113 ± 0.317	
012505M	121.95 ± 8.51	60.98 ± 4.26	53.12 ± 9.7	64.4 ± 4.38	11.28± 0.744	10.16± 0.67	3.648 ± 0.241	11.18 ± 0.682	
012505N	14.37 ± 1.35	7.19 ± 0.67	7.2 ± 1.47	7.95 ± 0.67	2.631± 0.127	2.368± 0.114	0.85 ± 0.041	2.608 ± 0.116	
012605E	33.75 ± 1.75	16.87 ± 0.88	11.62 ± 1.78	16.66 ± 0.83	4.701± 0.171	4.23± 0.153	1.52 ± 0.055	4.66 ± 0.156	
012605M	97.06 ± 2.63	48.53 ± 1.32	44.16 ± 3.1	51.97 ± 1.38	8.215± 0.203	7.393± 0.183	2.656 ± 0.066	8.143 ± 0.186	
012605N	9.24 ± 0.88	4.62 ± 0.44	3.25 ± 0.91	4.59 ± 0.42	1.881± 0.093	1.693± 0.083	0.608 ± 0.03	1.864 ± 0.085	
012705E	39.69 ± 1.76	19.84 ± 0.88	9.68 ± 1.67	18.07 ± 0.8	4.436± 0.2	3.993± 0.18	1.434 ± 0.065	4.398 ± 0.184	
012705M	50.9 ± 6.78	25.45 ± 3.39	29.82 ± 3.77	29.78 ± 2.37	2.862± 0.335	62.96± 3.685	22.62 ± 1.324	8.091 ± 0.443	
012705N	12.01 ± 1.16	6.01 ± 0.58	8.33 ± 1	7.52 ± 0.5	3.396± 0.16	3.056± 0.144	1.098 ± 0.052	3.366 ± 0.146	
012905E	42.11 ± 2.89	21.05 ± 1.44	16.28 ± 2.81	21.46 ± 1.34	4.921± 0.298	4.429± 0.268	1.591 ± 0.096	4.878 ± 0.273	
012905M	104.01 ± 31.5	52 ± 15.76	69.44 ± 36.81	64.07 ± 16.48	10.5± 2.626	9.454± 2.364	3.396 ± 0.849	10.41 ± 2.407	
012905N	20.9 ± 1.17	10.45 ± 0.58	6.61 ± 1.19	10.09 ± 0.56	2.699± 0.136	2.429± 0.123	0.873 ± 0.044	2.676 ± 0.125	
013005E	25.87 ± 1.41	12.93 ± 0.7	10.83 ± 1.36	13.5 ± 0.65	4.071± 0.158	3.664± 0.142	1.316 ± 0.051	4.036 ± 0.145	

Computed activity concentration of Radon Progeny and Equilibrium Activity Concentrations . . . Contd.

Sample code	218Po	214Pb	214Bi	EEC_{222}	212Pb	212Bi	208Tl	EEC_{220}	Remark
013005M	81.8 ± 4.83	40.9 ± 2.42	36.66 ± 5.47	43.59 ± 2.47	8.155± 0.38	7.339± 0.342	2.636 ± 0.123	8.084 ± 0.348	
013005N	10.48 ± 0.84	5.24 ± 0.42	2.46 ± 0.86	4.74 ± 0.4	1.333± 0.096	1.2± 0.086	0.431 ± 0.031	1.322 ± 0.088	
013105E	15.98 ± 1.41	7.99 ± 0.71	3.55 ± 1.35	7.15 ± 0.65	2.365± 0.158	2.128± 0.142	0.764 ± 0.051	2.344 ± 0.145	
013105M	69.16 ± 2.39	34.58 ± 1.19	35.8 ± 2.71	38.67 ± 1.22	7.379± 0.237	6.641± 0.213	2.385 ± 0.077	7.315 ± 0.217	
013105N	12.01 ± 0.98	6.01 ± 0.49	3.92 ± 1.03	5.84 ± 0.48	1.42± 0.099	1.278± 0.089	0.459 ± 0.032	1.408 ± 0.091	
010106E	19.97 ± 1.02	9.99 ± 0.51	3.34 ± 1.01	8.52 ± 1.1	2.091± 0.113	1.882± 0.102	0.676 ± 0.037	2.072 ± 0.104	
010106M	44.51 ± 2.23	22.25 ± 1.12	44.73 ± 2.4	33.11 ± 1.1	8.613± 0.245	7.752± 0.221	2.785 ± 0.079	8.538 ± 0.225	
010106N	10.78 ± 2.76	5.39 ± 1.38	3.42 ± 0.97	5.21 ± 0.85	1.7± 0.125	4.345± 1.778	1.561 ± 0.639	1.93 ± 0.192	
010206E	14.61 ± 3.91	7.31 ± 1.95	7.12 ± 1.65	8 ± 1.26	3.133± 0.237	10.29± 2.451	3.698 ± 0.88	3.756 ± 0.304	
010206M	80.38 ± 5.78	40.19 ± 2.89	44.6 ± 6.34	46.08 ± 2.89	8.293± 0.537	7.463± 0.484	2.681 ± 0.174	8.221 ± 0.492	
010206N	16.85 ± 3.32	8.43 ± 1.66	4.53 ± 1.1	7.83 ± 1.02	2.687± 0.127	5.903± 2.092	2.12 ± 0.752	2.967 ± 0.216	
010306E	24.81 ± 1.37	12.41 ± 0.69	11.12 ± 1.34	13.22 ± 0.64	3.44± 0.152	3.096± 0.137	1.112 ± 0.049	3.41 ± 0.14	
010306M	93.36 ± 7.29	46.68 ± 3.64	48.93 ± 2.84	52.44 ± 2.3	8.863± 0.277	13.14± 4.417	4.719 ± 1.586	3.422 ± 0.286	
010306N	30.51 ± 1.45	15.26 ± 0.73	7.7 ± 1.57	13.99 ± 0.72	4.51± 0.151	4.059± 0.136	1.458 ± 0.049	4.471 ± 0.138	
010406E	14.16 ± 1.1	7.08 ± 0.55	3.74 ± 1.05	6.56 ± 0.5	2.784 ± 0.128	2.505 ± 0.115	0.9 ± 0.041	2.76 ± 0.117	
010406M	103.04 ± 4.09	51.52 ± 2.05	40.63 ± 4.78	52.8 ± 2.14	9.361± 0.362	8.425± 0.326	3.026 ± 0.117	9.279 ± 0.332	
010406N	10.96 ± 0.93	5.48 ± 0.47	5.95 ± 0.98	6.23 ± 0.45	1.924± 0.102	1.732± 0.092	0.622 ± 0.033	1.908 ± 0.094	
010506E	28.85 ± 1.37	14.42 ± 0.69	10.19 ± 1.32	14.33 ± 0.63	4.318± 0.154	3.886± 0.138	1.396 ± 0.05	4.28 ± 0.141	
010506M	83.22 ± 1.57	41.61 ± 0.79	39.81 ± 1.87	45.3 ± 0.83	8.54± 0.137	7.686± 0.123	2.761 ± 0.044	8.466 ± 0.126	
010506N	6.3 ± 2.79	3.15 ± 1.39	8.93 ± 2.8	5.67 ± 1.31	3.462± 0.317	3.115± 0.285	1.119 ± 0.102	3.431 ± 0.291	
010606M	82.63 ± 6.86	41.31 ± 3.43	48.12 ± 2.2	48.23 ± 2.08	9.94± 0.181	9.222± 3.93	3.312 ± 1.412	9.877 ± 0.38	
010706N	25.16 ± 1.16	12.58 ± 0.58	9.47 ± 1.23	12.72 ± 0.57	4.295± 0.12	3.865± 0.108	1.388 ± 0.039	4.257 ± 0.11	
010706M	90.3 ± 9.38	45.15 ± 4.69	45.34 ± 11	49.96 ± 4.92	10.34± 0.843	9.309± 0.758	3.344 ± 0.272	10.25 ± 0.772	
010706E	25.32 ± 1.15	12.66 ± 0.58	9.36 ± 1.23	12.74 ± 0.56	4.134± 0.119	3.721± 0.107	1.336 ± 0.039	4.098 ± 0.109	

4.3 Comparison With Other Areas of the World

The indoor radon concentration determined in our lab is 23.9 Bq/m^3. It is about 38.5% less than the global average 39 Bq/m^3 reported by WHO [WHO, 2005]

Table 4.3: Comparison of Indoor Radon Concentrations

Region	Country	Population In 1996 (10^6)	Mean Radon concentration (Bqm^{-3})
Africa	Algeria	28.78	30
	Egypt	63.27	9
	Ghana	17.83	
America	Canada	29.68	34
	United States	269.4	46
	Argentina	35.22	37
	Chile	14.42	25
	Paraguay	4.96	28
Asia	China	1232	24
	Honk Kong	6.19	41
	India	944.6	57
	Indonesia	200.45	12
	Japan	125.4	16
	Iran	69.98	82
	Kuwait	1.69	14
	Syria	14.57	44
Europe	Denmark	5.24	53
	Estonia	1.47	120
	Finland	5.13	120
	Belgium	10.16	48
	France	58.33	62
	Germany	81.92	50 9
	Ireland	3.55	
	Czech Republic	10.25	140
	Hungary	10.05	107
	Albania	3.4	120
	Croatia	4.5	35
	Slovenia	1.92	87
	Spain	39.67	86

4.4 Diurnal variation of EEC of ^{222}Rn and ^{220}Rn

The diurnal variation of EEC ^{222}Rn and ^{220}Rn is due to atmospheric mixing phenomena. During the day time solar heating tends to induce some turbulence. This results easy transportation of radon upwards. At night and in the morning hours, the atmosphere mixup will be minimum which will trap radon to the ground. This phenomena results in that the EEC concentration will be maximum in the morning and minimum during day time.

From the datas collected in this experiment, the EEC variation of ^{222}Rn and ^{220}Rn was analyzed. The results obtained are shown in table 4.4 and the corresponding plot is shown in fig. 4.2 and fig. 4.3.

Table 4.4: Diurnal Variation of Equilibrium Equivalent Concentration of ^{222}Rn & ^{220}Rn

Date	EEC_{222}			EEC_{220}			Remark
	M.	N.	E.	M.	N.	E.	
20-May-06	40.59	5.49	10.48	6.83	2.30	3.69	
21-May-06	8.81	11.78	36.52	1.92	4.24	8.18	Room Open overnight
22-May-06	65.94			10.46			
24-May-06	81.17		15.22	14.24		4.66	
25-May-06	64.40	7.95	35.13	11.18	2.61	8.11	
26-May-06	51.97	4.59	16.66	8.14	1.86	4.66	
27-May-06	29.78	7.52	18.07	8.09	3.37	4.40	
29-May-06	64.07	10.09	21.46	10.41	2.68	4.88	
30-May-06	43.59	4.74	13.50	8.08	1.32	4.04	
31-May-06	38.67	5.84	7.15	7.32	1.41	2.34	
1-Jun-06	33.11	5.21	8.52	8.54	1.93	2.07	
2-Jun-06	46.08	7.83	8.00	8.22	2.97	3.76	
3-Jun-06	52.44	13.99	13.22	3.42	4.47	3.41	Heavy rain in the afternoon
4-Jun-06	52.80	6.23	6.56	9.28	1.91	2.76	
5-Jun-06	45.30	5.67	14.33	8.47	3.43	4.28	
6-Jun-06	48.23			9.88			
7-Jun-06	49.96	12.72	12.74	10.25	4.26	4.10	
Min	8.81	4.59	6.56	1.92	1.32	2.07	
Max	81.17	13.99	36.52	14.24	4.47	8.18	
Average	48.05	7.83	15.84	8.51	2.77	4.36	
st. deviation	15.86	3.00	8.82	2.73	1.02	1.69	

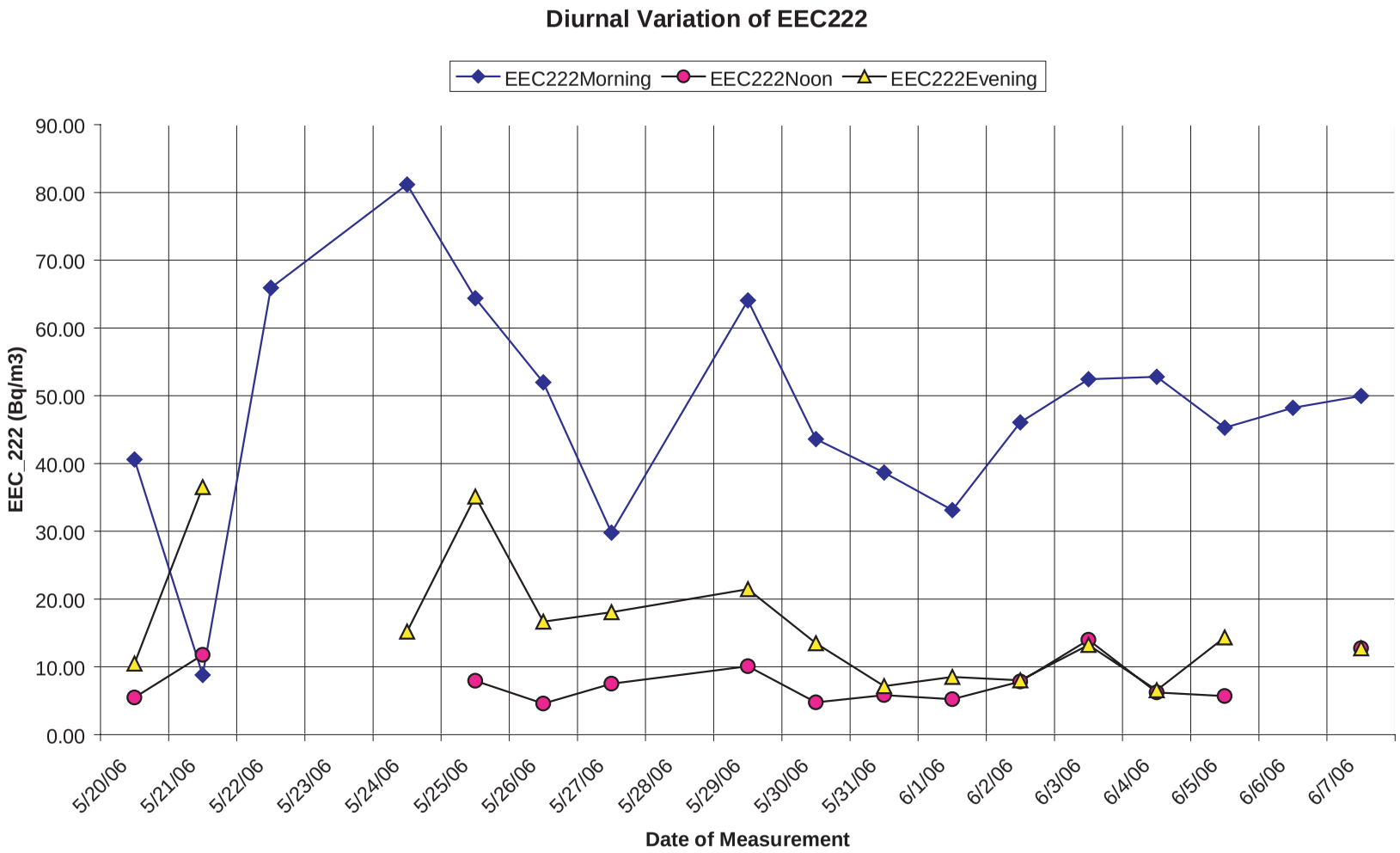

Figure 4.2: Diurnal Variation of EEC of ^{222}Rn

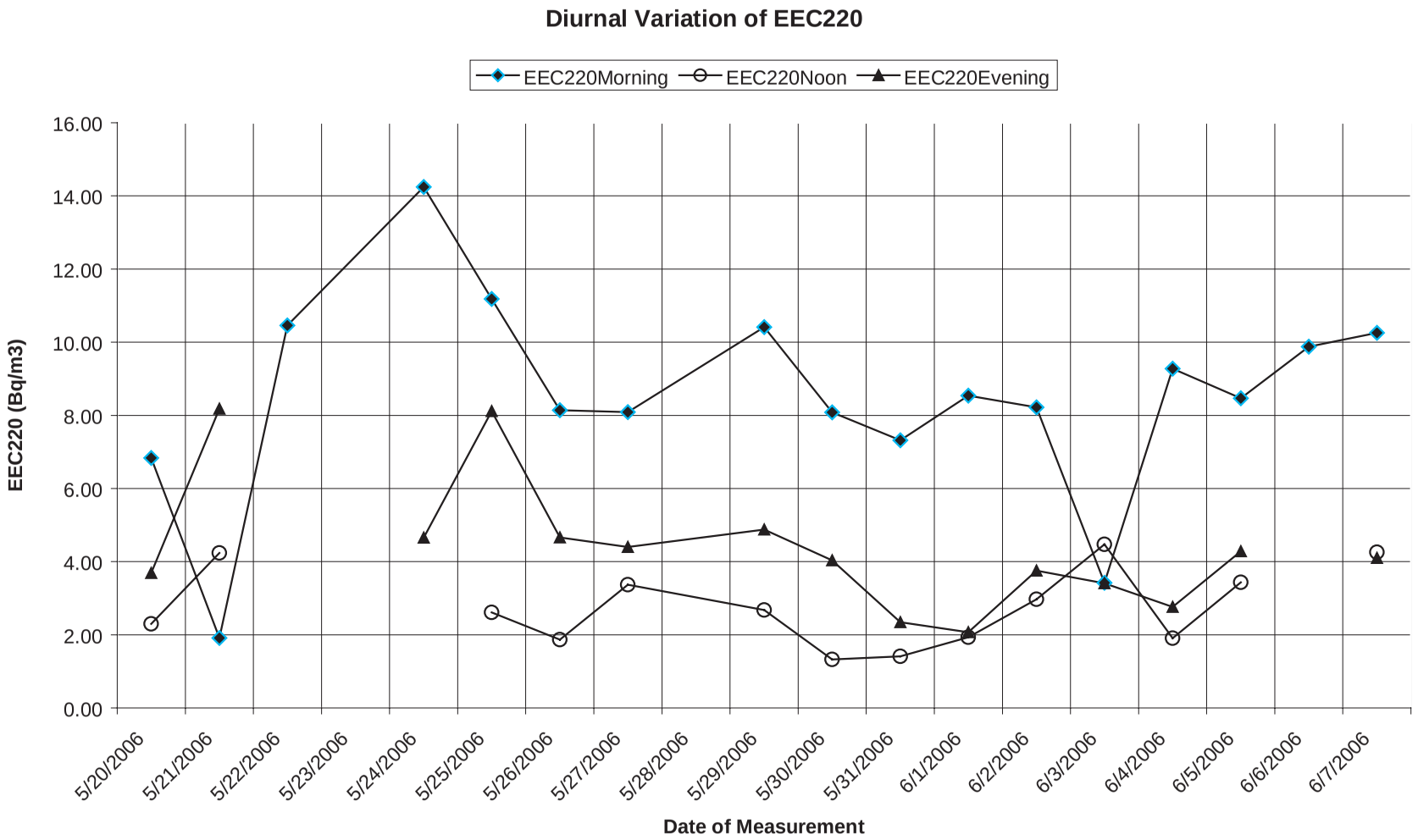

Figure 4.3: Diurnal Variation of EEC of ^{220}Rn

This results were compared with other results [Winkler, 2001] and [Liguo, 2004]. It showed a good agreement in that the EEC concentration for both ^{222}Rn and ^{220}Rn has a maximum during early morning, and minimum at noon. This result is also in good agreement with the theory explained in the beginning of this section.

Chapter 5

Conclusion

In this work, the method of defined solid angle absolute beta counting, using an end-window Geiger-Müller counter, was tried and tested for the first time in the nuclear science laboratory of the physics department. In view of the portability and low cost aspect of the method it is promising for future wide area survey of radon.

Using the above method concentration of radon progeny and EEC of ^{222}Rn and ^{220}Rn was determined. The diurnal variation of the EEC concentration of ^{222}Rn and ^{220}Rn was studied and the results obtained are in agreement with earlier works in other parts of the world.

In the future, this method may be used to study various aspects of radon and thoron concentrations in air. Some potential areas of research include:

- Radon concentration in various parts of the country (emphasis on mining areas);
- Seasonal variation of radon and radon progeny concentration at locations of interest;
- Radon and progeny measurement in all parts of Ethiopia so as to establish "Radon map of Ethiopia";
- Earth quake prediction in places which are exposed to it as sudden change in radon concentration can be related to turbulence inside the earth's crust.

Improvements Proposed on the Method

The method of data acquisition may be improved by automation. i.e. the count of the GM tube may be directly fed, with a suitably designed interface, to a computer in a progressively increasing interval of time rather than manual counting. This simplifies and slashes the time required to feed the gross count of hundreds of intervals manually and thereby reduce the labor required to analyze the data.

Improving the shielding of the detection system may also help to minimize the variation of the background radiation.

Bibliography

Gil Hoon Ahn and Jai-Ki Lee. Construction of an environmental radon monitoring system using cr-39 nuclear track detectors. *Nuclear engineering and technology*, 37(4):395–400, 2005.

Al-Kazwini T Akeel and Mahmoud A Hasan. Radon concentration in jordanian drinking water and hot springs. *Journal of radiological protection*, 23:439–448, 2003.

A. Al-Sharif and Y.S. Abelrahman. Factors affecting radon concentration in houses. *Turk journal of physics*, (25):153–158, 2001.

M.E. Bacon. A comparison of electrostatic and filtered air collection of radon progeny. *European Journal of Physics*, 25:239–248, 2004.

B.P. Burtt. Absolute beta count. *Nucleonics*, 5(2):28–43, 1949.

Samuelsson Christer. *Radiation at home,outdoors and in the workplace*. Scandnavian science publisher,Oslo, 2001.

K.D. Cliff. Assessment of airborne radon daughter concentrations in dwellings in great britain. *Phys. Med. Biol.*, 23, 1978.

Jeffery Codore. Ionizing radiation. MIT Lecture Note on Ionizing Radiation, 2003.

EPA. Indoor radon and radon decay product measurement device protocols. Technical report, U.S. Environmental Protection Agency, 1992.

EPA. EPA a citizen's guide to radon. Technical report, U.S. environmental protection agency, September 2005.

G. F. Knoll. *Radiation Detection and Measurement*. John wiley and sons,Inc., third edition, 2000.

Ralph E. Lapp and Andrews Howard L. *Nuclear Radiation Physics*. Prentice-Hall,Inc„ fourth edition, 1972. ISBN 0-13-625988-x.

William R. Leo. *Tehniques for nuclear and Particle Physics Experiments*. Springer-verlag, second edition, 1994. ISBN 3-540-57280-5.

Zhang Liguo. Atmospheric radon levels in beijing, china. *Radiation Protection Dosimetry*, 112(3):449–453, 2004.

A. Nagaratnam. Radon : A historical overiew. *Bulletin of Radiation Protection*, 17 (3 and 4):1–9, 1994.

National Research Council. Health effects of exposure to radon: Beir vi. Report, Committee on Health Risks of Exposure to Radon(BEIR VI, Board on Radiation Effects Research , Commission on life Sciences,National Resarch Council, 1999.

Z. Papp. Defined solid angle absolute β-counting for use in the radioanalysis of environmental samples. *Journal of Radioanalytical and Nuclear Chemistry*, 222 (1-2):157–163, 1997.

Z. Papp and S. Daróczy. Measurement of radon decay products and thoron decay products in air by beta counting using end-window gieger-muller counter. *Health Physics*, 72(4):601–610, 1997.

Otto G. Raabe and McDonald E.Wrenn. Analysis of the activity of radon daughter samples by weighted least squares. *Health Physics Pregamon Press*, 17:593–605, 1969.

R.M. Singru. *Experimental Nuclear physics*. Wiley Eastern private limited, 1974. ISBN 0-85226-822-x.

Anastasiou Tassos and Tsertos Haralabos. Indoor radon (Rn-222) concentration measurements in cyprus using high-sensitivity portable detectors. *Ucy-Phy-02/04*, pages 1–21, 2003.

UNSCEAR. Sources and effects of radiation united nations scientific committee on the effects of atomic radiation unscear 2000 report to the general assembly,with scientific annexes. Report, United Nation Scientific Committee on the effects of Atomic radiation (UNSCEAR), 2000.

WHO. WHO fact sheet no.291, June 2005.

R. Winkler. Diurnal and seasonal variation of the equilibrium state between short-lived radon decay products and radon gas in ground-level air. *Radiat Environ Biophysics*, 40:115–123, 2001.

DECLARATION

I the under signed declare that the thesis is my original work, has not been presented for a degree in any other university and that all sources of material used for the thesis have been duly acknowledged.

Name: _____

Signature: _____

This Thesis has been submitted for examination with my approval as university advisor.

Name: _____

Signature: _____